

# Systematic study of the strong decays of the $P_c$ states and their possible isospin cousins via the QCD sum rules\*

Xiu-Wu Wang (王修武)<sup>†</sup> Xin Li (李欣) Zhi-Gang Wang (王志刚)<sup>‡</sup>

Department of Physics, North China Electric Power University, Baoding 071003, P. R. China

**Abstract:** In the present work, the strong decays of the discovered  $P_c(4380)$ ,  $P_c(4440)$ ,  $P_c(4457)$  and their possible isospin cousins are systematically studied via the assignment that they are meson-baryon molecular states. In detail, the strong decay constants and partial decay widths of their decay channels are calculated under the framework of QCD sum rules. The decay widths of the discovered  $P_c(4380)$ ,  $P_c(4440)$ , and  $P_c(4457)$  are in good agreement with the experiments. The predictions of the decays of these three related possible isospin cousins are presented, which would shed light on their findings in experiments. In return, this may testify to the assignments of the discovered  $P_c$  states.

**Keywords:** Strong decays, pentaquark molecular states, QCD sum rules

**DOI:** 10.1088/1674-1137/ae66d1 **CSTR:**

## I. INTRODUCTION

So far, the LHCb collaboration has discovered the following exotic  $P_c$  states composed of five valence quarks: the  $P_c(4380)$ , observed in 2015 through analysis of the  $\Lambda_b^0 \rightarrow J/\psi K^- p$  decays [1]; the  $P_c(4312)$ ,  $P_c(4440)$ , and  $P_c(4457)$ , found in 2019 in the  $J/\psi p$  mass spectrum [2]; and the  $P_c(4337)$ , in the  $J/\psi p$  and  $J/\psi \bar{p}$  systems in the  $B_s^0 \rightarrow J/\psi p \bar{p}$  decays [3]. It is worth mentioning that the  $P_c(4380)$  has neither been confirmed nor conclusively excluded in subsequent investigations. For the  $P_c(4337)$ , it is difficult to assign it as a molecular state due to a lack of nearby meson-baryon thresholds; furthermore, its existence still requires confirmation. The strong decay of the  $P_c(4312)$  has been fully analyzed in Ref. [4] by our group. Thus, the present work focuses on the strong decays of the observed  $P_c(4380)$ ,  $P_c(4440)$ , and  $P_c(4457)$ . It should be noted that the  $P_c(4380)$ , having a broad width, remains a controversial subject, as its existence was neither confirmed nor refuted in the updated analysis. In 2019, a clear signal for this state was not observed in the  $J/\psi p$  mass spectrum by the LHCb group [2]; therefore, its existence needs further experimental confirmation. In the present study, we still treat it as the ' $P_c(4380)$ ' state with the mass and width proposed by LHCb in 2015 [1] for the systematic study of these discovered  $P_c$  states un-

der the meson-baryon molecular picture. Moreover, the predictions of the decays for this controversial state, derived in the present work, may provide a reference for its further experimental confirmation in the future. The Breit-Wigner masses and widths of the  $P_c(4380)$ ,  $P_c(4440)$ , and  $P_c(4457)$  are listed in [1, 2].

$$\begin{aligned}
 P_c(4380) : M &= 4380 \pm 8 \pm 29 \text{ MeV}, \\
 \Gamma &= 205 \pm 18 \pm 86 \text{ MeV}, \\
 P_c(4440) : M &= 4440.3 \pm 1.3^{+4.1}_{-4.7} \text{ MeV}, \\
 \Gamma &= 20.6 \pm 4.9^{+8.7}_{-10.1} \text{ MeV}, \\
 P_c(4457) : M &= 4457.3 \pm 0.6^{+4.1}_{-1.7} \text{ MeV}, \\
 \Gamma &= 6.4 \pm 2.0^{+5.7}_{-1.9} \text{ MeV}. \tag{1}
 \end{aligned}$$

Via the experiments [1, 2], one could determine that the isospin of  $P_c(4380)$ ,  $P_c(4440)$ , and  $P_c(4457)$  is  $\frac{1}{2}$ . Since the spins and parities of these  $P_c$  states have not been definitively determined experimentally yet, theoretical groups have different arguments about their physical natures, which will surely deepen our understanding of the non-perturbative behavior of strong interactions. This is still a hotly debated and open question. Based on the

Received 23 January 2026; Accepted 29 April 2026

\* This work is supported by the National Natural Science Foundation with Grant Number 12575083 and the Natural Science Foundation of Hebei Province with Grant Number A2024502002

<sup>†</sup> E-mail: wangxiuwu2020@163.com

<sup>‡</sup> E-mail: zgwang@aliyun.com



Content from this work may be used under the terms of the Creative Commons Attribution 3.0 licence. Any further distribution of this work must maintain attribution to the author(s) and the title of the work, journal citation and DOI. Article funded by SCOAP<sup>3</sup> and published under licence by Chinese Physical Society and the Institute of High Energy Physics of the Chinese Academy of Sciences and the Institute of Modern Physics of the Chinese Academy of Sciences and IOP Publishing Ltd

fact that the masses of these  $P_c$  states are just below the thresholds of the  $\Sigma_c^{(*)}\bar{D}^{(*)}$  pairs, a typical interpretation is that they are the S-wave hidden-charm meson-baryon molecules [5–19]. Another typical assignment is that they are the compact pentaquark states [20–28]. In the molecular picture, it is widely accepted that the  $J^P$  of  $P_c(4312)$  is  $\frac{1}{2}^-$ . The divergences mainly come from the other  $P_c$  states; for example,  $P_c(4440)$  and  $P_c(4457)$  are assigned as the  $\Sigma_c\bar{D}^*$  molecules with  $J^P$  being  $\frac{1}{2}^-$  and  $\frac{3}{2}^-$  in Refs. [5, 29, 30], respectively. However, in Refs. [31–34], their  $J^P$  are attributed as  $\frac{3}{2}^-$  and  $\frac{1}{2}^-$ , respectively. As for our argument for the  $P_c(4312)$ ,  $P_c(4380)$ ,  $P_c(4440)$ , and  $P_c(4457)$ , considering these  $P_c$  states were discovered in the  $J/\psi p$  invariant mass spectrum, their isospins should be  $I = \frac{1}{2}$  via the conservation of the isospins in the strong interactions [39]. Thus, we constructed currents with high and low isospins for the first time to interpolate the hidden-charm  $P_c$  states under the framework of the QCD sum rules to avoid pollution between high and low isospin states. The study nicely assigns the  $P_c(4312)$ ,  $P_c(4380)$ ,  $P_c(4440)$ , and  $P_c(4457)$  as the  $\bar{D}\Sigma_c$ ,  $\bar{D}\Sigma_c^*$ ,  $\bar{D}^*\Sigma_c$ , and  $\bar{D}^*\Sigma_c^*$  molecular states with their  $J^P$  being  $\frac{1}{2}^-$ ,  $\frac{3}{2}^-$ ,  $\frac{3}{2}^-$ , and  $\frac{5}{2}^-$ , respectively. Moreover, four high isospin cousins of the  $P_c(4312)$ ,  $P_c(4380)$ ,  $P_c(4440)$ , and  $P_c(4457)$  are predicted as the  $\bar{D}\Sigma_c$ ,  $\bar{D}\Sigma_c^*$ ,  $\bar{D}^*\Sigma_c$ , and  $\bar{D}^*\Sigma_c^*$  resonance states. For more insights on these  $P_c$  states, one can check the relevant reviews in Refs. [35–38]. Motivated by these heated debates regarding the nature of these  $P_c$  states, we turn our attention to their strong decays and try to find more information to determine their natures.

The mass and width are two basic parameters to determine the physical nature of a hadronic state. Many theoretical groups have applied different methods to study their masses [5–13, 20, 21, 39–41] and strong decays [19, 29, 30, 42–45] under the physical picture of meson-baryon hadronic molecules. For the strong decay, the isospin, spin, and parity should be conserved; different  $IJ^P$  result in different decay modes. In our previous work, the masses of the observed  $P_c$  and  $P_{cs}$  are studied by clearly differentiating the isospins of the currents interpolating the exotic states for the first time in a comprehensive way [39, 46]. Results show that the mass of the high isospin state is several dozen MeV above that of the low one, which is solid proof of the necessity to differentiate the isospins to avoid pollution between the high and low isospins in studying these  $P_c$  and  $P_{cs}$  states. Hence, the necessity to study the strong decay of the possible high isospin cousins of these  $P_c$  and  $P_{cs}$  is also obvious. Their observation in the predicted decay modes would shed light on the nature of the  $P_c$  states in return. Furthermore, the  $J^P$  and pole residues are also derived [39, 46], ready for the present work to study the strong decays.

The article is arranged as follows: The QCD sum rules for the strong decays of  $P_c(4380)$ ,  $P_c(4410)$ ,

$P_c(4440)$ ,  $P_c(4470)$ ,  $P_c(4457)$ , and  $P_c(4620)$  are derived in Sect. 2. The numerical results and discussions are presented in Sect. 3, and Sect. 4 is reserved for the conclusions of the present study.

## II. QCD SUM RULES FOR STRONG DECAYS OF THE PENTAQUARK MOLECULAR STATES

Following the results derived in Ref. [39], the quantum numbers  $(I, J^P)$  of the  $P_c(4380)$ ,  $P_c(4440)$ , and  $P_c(4457)$  are  $(\frac{1}{2}, \frac{3}{2}^-)$ ,  $(\frac{1}{2}, \frac{3}{2}^-)$ , and  $(\frac{1}{2}, \frac{5}{2}^-)$ , respectively. The three possible corresponding isospin cousins of  $P_c(4380)$ ,  $P_c(4440)$ , and  $P_c(4457)$  are  $P_c(4410)$ ,  $P_c(4470)$ , and  $P_c(4620)$ , with their  $(I, J^P)$  quantum numbers assigned as  $(\frac{3}{2}, \frac{3}{2}^-)$ ,  $(\frac{3}{2}, \frac{3}{2}^-)$ , and  $(\frac{3}{2}, \frac{5}{2}^-)$ , respectively. The  $(I, J^P)$  for  $N$ ,  $\Delta$ ,  $\eta_c$ , and  $J/\psi$  are  $(\frac{1}{2}, \frac{1}{2}^+)$ ,  $(\frac{3}{2}, \frac{3}{2}^+)$ ,  $(0, 0^-)$ , and  $(0, 1^-)$ , respectively. Considering the conservation of isospin  $I$  in the strong decays, the following decay channels are studied in the present work.

$$\begin{aligned}
P_c(4380) &\rightarrow \eta_c + N, \\
P_c(4380) &\rightarrow J/\psi + N, \\
P_c(4410) &\rightarrow \eta_c + \Delta, \\
P_c(4410) &\rightarrow J/\psi + \Delta, \\
P_c(4440) &\rightarrow \eta_c + N, \\
P_c(4440) &\rightarrow J/\psi + N, \\
P_c(4470) &\rightarrow \eta_c + \Delta, \\
P_c(4470) &\rightarrow J/\psi + \Delta, \\
P_c(4457) &\rightarrow \eta_c + N, \\
P_c(4457) &\rightarrow J/\psi + N, \\
P_c(4620) &\rightarrow \eta_c + \Delta, \\
P_c(4620) &\rightarrow J/\psi + \Delta, \tag{2}
\end{aligned}$$

where the proton is marked as  $N$  to avoid confusion with the four-momentum  $p_\mu$ . The currents  $\mathcal{J}_{\eta_c}(x)$ ,  $\mathcal{J}_{J/\psi,\mu}(x)$ ,  $\mathcal{J}_N(x)$ ,  $\mathcal{J}_{\Delta,\mu}(x)$ ,  $\mathcal{J}_{P_{A,\mu}}(x)$ ,  $\mathcal{J}_{P_{B,\mu}}(x)$ ,  $\mathcal{J}_{P_{C,\mu}}(x)$ ,  $\mathcal{J}_{P_{D,\mu}}(x)$ ,  $\mathcal{J}_{P_{E,\mu\nu}}(x)$ , and  $\mathcal{J}_{P_{F,\mu\nu}}(x)$  are applied to interpolate the  $\eta_c$ ,  $J/\psi$ ,  $N$ ,  $\Delta$ ,  $P_c(4380)$ ,  $P_c(4410)$ ,  $P_c(4440)$ ,  $P_c(4470)$ ,  $P_c(4457)$ , and  $P_c(4620)$ , respectively. For convenience,  $P_{A\sim F}$  are used to represent the states  $P_c(4380)$ ,  $P_c(4410)$ ,  $P_c(4440)$ ,  $P_c(4470)$ ,  $P_c(4457)$ , and  $P_c(4620)$ , respectively. The mentioned currents are expressed as follows:

$$\mathcal{J}_{\eta_c}(x) = \bar{c}(x)i\gamma_5 c(x), \tag{3}$$

$$\mathcal{J}_{J/\psi,\mu}(x) = \bar{c}(x)\gamma_\mu c(x), \tag{4}$$

$$\mathcal{J}_N(x) = \varepsilon^{ijk} u^{iT}(x) C \gamma_\alpha u^j(x) \gamma^\alpha \gamma_5 d^k(x), \quad (5)$$

$$\Pi_{\mu,1}(p, q) = i^2 \int d^4x d^4y e^{ip \cdot x} e^{iq \cdot y} \langle 0 | T \{ \mathcal{J}_{\eta_c}(x) \mathcal{J}_N(y) \bar{\mathcal{J}}_{P_{A,\mu}}(0) \} | 0 \rangle, \quad (13)$$

$$\mathcal{J}_{\Delta,\mu}(x) = \frac{1}{\sqrt{3}} \varepsilon^{ijk} u^{iT}(x) C \gamma_\mu u^j(x) d^k(x) + \sqrt{\frac{2}{3}} \varepsilon^{ijk} u^{iT}(x) C \gamma_\mu d^j(x) u^k(x), \quad (6)$$

$$\Pi_{\mu\zeta,2}(p, q) = i^2 \int d^4x d^4y e^{ip \cdot x} e^{iq \cdot y} \langle 0 | T \{ \mathcal{J}_{J/\psi,\zeta}(x) \mathcal{J}_N(y) \bar{\mathcal{J}}_{P_{A,\mu}}(0) \} | 0 \rangle, \quad (14)$$

$$\mathcal{J}_{P_{A,\mu}}(x) = \frac{1}{\sqrt{3}} \bar{c}(x) i \gamma_5 u(x) \varepsilon^{ijk} u^{iT}(x) C \gamma_\mu d^j(x) c^k(x) - \sqrt{\frac{2}{3}} \bar{c}(x) i \gamma_5 d(x) \varepsilon^{ijk} u^{iT}(x) C \gamma_\mu u^j(x) c^k(x), \quad (7)$$

$$\Pi_{\mu\chi,3}(p, q) = i^2 \int d^4x d^4y e^{ip \cdot x} e^{iq \cdot y} \langle 0 | T \{ \mathcal{J}_{\eta_c}(x) \mathcal{J}_{\Delta,\chi}(y) \bar{\mathcal{J}}_{P_{B,\mu}}(0) \} | 0 \rangle, \quad (15)$$

$$\mathcal{J}_{P_{B,\mu}}(x) = \sqrt{\frac{2}{3}} \bar{c}(x) i \gamma_5 u(x) \varepsilon^{ijk} u^{iT}(x) C \gamma_\mu d^j(x) c^k(x) + \frac{1}{\sqrt{3}} \bar{c}(x) i \gamma_5 d(x) \varepsilon^{ijk} u^{iT}(x) C \gamma_\mu u^j(x) c^k(x), \quad (8)$$

$$\Pi_{\mu\chi\zeta,4}(p, q) = i^2 \int d^4x d^4y e^{ip \cdot x} e^{iq \cdot y} \langle 0 | T \{ \mathcal{J}_{J/\psi,\zeta}(x) \mathcal{J}_{\Delta,\chi}(y) \bar{\mathcal{J}}_{P_{B,\mu}}(0) \} | 0 \rangle. \quad (16)$$

$$\mathcal{J}_{P_{C,\mu}}(x) = \frac{1}{\sqrt{3}} \bar{c}(x) \gamma_\mu u(x) \varepsilon^{ijk} u^{iT}(x) C \gamma_\nu d^j(x) \gamma^\nu \gamma_5 c^k(x) - \sqrt{\frac{2}{3}} \bar{c}(x) \gamma_\mu d(x) \varepsilon^{ijk} u^{iT}(x) C \gamma_\nu u^j(x) \gamma^\nu \gamma_5 c^k(x), \quad (9)$$

$$\Pi_{\mu,5}(p, q) = i^2 \int d^4x d^4y e^{ip \cdot x} e^{iq \cdot y} \langle 0 | T \{ \mathcal{J}_{\eta_c}(x) \mathcal{J}_N(y) \bar{\mathcal{J}}_{P_{C,\mu}}(0) \} | 0 \rangle, \quad (17)$$

$$\mathcal{J}_{P_{D,\mu}}(x) = \sqrt{\frac{2}{3}} \bar{c}(x) \gamma_\mu u(x) \varepsilon^{ijk} u^{iT}(x) C \gamma_\nu d^j(x) \gamma^\nu \gamma_5 c^k(x) + \frac{1}{\sqrt{3}} \bar{c}(x) \gamma_\mu d(x) \varepsilon^{ijk} u^{iT}(x) C \gamma_\nu u^j(x) \gamma^\nu \gamma_5 c^k(x), \quad (10)$$

$$\Pi_{\mu\zeta,6}(p, q) = i^2 \int d^4x d^4y e^{ip \cdot x} e^{iq \cdot y} \langle 0 | T \{ \mathcal{J}_{J/\psi,\zeta}(x) \mathcal{J}_N(y) \bar{\mathcal{J}}_{P_{C,\mu}}(0) \} | 0 \rangle, \quad (18)$$

$$\mathcal{J}_{P_{E,\mu\nu}}(x) = \frac{1}{\sqrt{3}} \bar{c}(x) \gamma_\mu u(x) \varepsilon^{ijk} u^{iT}(x) C \gamma_\nu d^j(x) c^k(x) - \sqrt{\frac{2}{3}} \bar{c}(x) \gamma_\mu d(x) \varepsilon^{ijk} u^{iT}(x) C \gamma_\nu u^j(x) c^k(x) + (\mu \leftrightarrow \nu), \quad (11)$$

$$\Pi_{\mu\chi,7}(p, q) = i^2 \int d^4x d^4y e^{ip \cdot x} e^{iq \cdot y} \langle 0 | T \{ \mathcal{J}_{\eta_c}(x) \mathcal{J}_{\Delta,\chi}(y) \bar{\mathcal{J}}_{P_{D,\mu}}(0) \} | 0 \rangle, \quad (19)$$

$$\mathcal{J}_{P_{F,\mu\nu}}(x) = \sqrt{\frac{2}{3}} \bar{c}(x) \gamma_\mu u(x) \varepsilon^{ijk} u^{iT}(x) C \gamma_\nu d^j(x) c^k(x) + \frac{1}{\sqrt{3}} \bar{c}(x) \gamma_\mu d(x) \varepsilon^{ijk} u^{iT}(x) C \gamma_\nu u^j(x) c^k(x) + (\mu \leftrightarrow \nu), \quad (12)$$

$$\Pi_{\mu\chi\zeta,8}(p, q) = i^2 \int d^4x d^4y e^{ip \cdot x} e^{iq \cdot y} \langle 0 | T \{ \mathcal{J}_{J/\psi,\zeta}(x) \mathcal{J}_{\Delta,\chi}(y) \bar{\mathcal{J}}_{P_{D,\mu}}(0) \} | 0 \rangle. \quad (20)$$

$$\Pi_{\mu\nu,9}(p, q) = i^2 \int d^4x d^4y e^{ip \cdot x} e^{iq \cdot y} \langle 0 | T \{ \mathcal{J}_{\eta_c}(x) \mathcal{J}_N(y) \bar{\mathcal{J}}_{P_{E,\mu\nu}}(0) \} | 0 \rangle, \quad (21)$$

where  $C$  is the charge conjugation matrix,  $\varepsilon^{ijk}$  represents the antisymmetric tensor, and  $i, j$ , and  $k$  are the color indices. Following previous works, the three-point correlation functions in the QCD sum rules are constructed to study the related strong decays.

$$\Pi_{\mu\nu\zeta,10}(p, q) = i^2 \int d^4x d^4y e^{ip \cdot x} e^{iq \cdot y} \langle 0 | T \{ \mathcal{J}_{J/\psi,\zeta}(x) \mathcal{J}_N(y) \bar{\mathcal{J}}_{P_{E,\mu\nu}}(0) \} | 0 \rangle, \quad (22)$$

$$\begin{aligned} & \Pi_{\mu\nu\chi,11}(p, q) \\ &= i^2 \int d^4x d^4y e^{ip \cdot x} e^{iq \cdot y} \langle 0 | T \{ \mathcal{J}_{\eta_c}(x) \mathcal{J}_{\Delta, \chi}(y) \bar{\mathcal{J}}_{P_F, \mu\nu}(0) \} | 0 \rangle, \end{aligned} \quad (23)$$

$$\begin{aligned} & \Pi_{\mu\nu\chi\zeta,12}(p, q) \\ &= i^2 \int d^4x d^4y e^{ip \cdot x} e^{iq \cdot y} \langle 0 | T \{ \mathcal{J}_{J/\psi, \zeta}(x) \mathcal{J}_{\Delta, \chi}(y) \bar{\mathcal{J}}_{P_F, \mu\nu}(0) \} | 0 \rangle, \end{aligned} \quad (24)$$

where  $T$  is the time order operator, and  $i^2 = -1$ . On the hadronic side, the complete sets of intermediate hadron states with the same quantum numbers as the currents  $\mathcal{J}_{\eta_c}(x)$ ,  $\mathcal{J}_{J/\psi, \mu}(x)$ ,  $\mathcal{J}_N(x)$ ,  $\mathcal{J}_{\Delta, \mu}(x)$ , and  $\mathcal{J}_{P_{A-F}}(x)$  are routinely inserted into those three-point correlation functions, and the contributions of the ground states are isolated. Thus, the correlation functions on the hadronic side are given by

$$\Pi_{\mu,1}(p, q) = \frac{f_{\eta_c} m_{\eta_c}^2}{2m_c} \lambda_N \lambda_{P_A} g_{\eta_c N,1} \times \frac{u(q) \bar{u}(q) i \gamma_5 U_\alpha(p') \bar{U}_\mu(p') p^\alpha}{(m_{P_A}^2 - p'^2) (m_{\eta_c}^2 - p^2) (m_N^2 - q^2)} + \dots, \quad (25)$$

$$\Pi_{\mu\zeta,2}(p, q) = f_{J/\psi} m_{J/\psi} \lambda_N \lambda_{P_A} \frac{-i g_{J/\psi N,2} u(q) \bar{u}(q) U_\alpha(p') \bar{U}_\mu(p') \varepsilon_\zeta(p) \varepsilon^{*\alpha}(p)}{(m_{P_A}^2 - p'^2) (m_{J/\psi}^2 - p^2) (m_N^2 - q^2)} + \dots, \quad (26)$$

$$\Pi_{\mu\chi,3}(p, q) = -\frac{f_{\eta_c} m_{\eta_c}^2}{2m_c} \lambda_\Delta \lambda_{P_B} g_{\eta_c \Delta,3} \frac{u_\chi(q) \bar{u}_\beta(q) U^\beta(p') \bar{U}_\mu(p')}{(m_{P_B}^2 - p'^2) (m_{\eta_c}^2 - p^2) (m_\Delta^2 - q^2)} + \dots, \quad (27)$$

$$\Pi_{\mu\chi\zeta,4}(p, q) = f_{J/\psi} m_{J/\psi} \lambda_\Delta \lambda_{P_B} g_{J/\psi \Delta,4} \cdot \frac{u_\chi(q) \bar{u}_\beta(q) \gamma^5 \gamma^\alpha U_\beta(p') \bar{U}_\mu(p') \varepsilon_\zeta(p) \varepsilon^{*\alpha}(p)}{(m_{P_B}^2 - p'^2) (m_{J/\psi}^2 - p^2) (m_\Delta^2 - q^2)} + \dots, \quad (28)$$

$$\Pi_{\mu,5}(p, q) = \frac{f_{\eta_c} m_{\eta_c}^2}{2m_c} \lambda_N \lambda_{P_C} g_{\eta_c N,5} \frac{u(q) \bar{u}(q) i \gamma^5 U_\alpha(p') \bar{U}_\mu(p') p^\alpha}{(m_{P_C}^2 - p'^2) (m_{\eta_c}^2 - p^2) (m_N^2 - q^2)} + \dots, \quad (29)$$

$$\Pi_{\mu\zeta,6}(p, q) = -f_{J/\psi} m_{J/\psi} \lambda_N \lambda_{P_C} g_{J/\psi N,6} \frac{u(q) \bar{u}(q) U_\alpha(p') \bar{U}_\mu(p') \varepsilon_\zeta(p) \varepsilon^{*\alpha}(p)}{(m_{P_C}^2 - p'^2) (m_{J/\psi}^2 - p^2) (m_N^2 - q^2)} + \dots, \quad (30)$$

$$\Pi_{\mu\chi,7}(p, q) = \frac{f_{\eta_c} m_{\eta_c}^2}{2m_c} \lambda_\Delta \lambda_{P_D} g_{\eta_c \Delta,7} \frac{i u_\chi(q) \bar{u}_\beta(q) U^\beta(p') \bar{U}_\mu(p')}{(m_{P_D}^2 - p'^2) (m_{\eta_c}^2 - p^2) (m_\Delta^2 - q^2)} + \dots, \quad (31)$$

$$\Pi_{\mu\chi\zeta,8}(p, q) = f_{J/\psi} m_{J/\psi} \lambda_\Delta \lambda_{P_D} g_{J/\psi \Delta,8} \cdot \frac{u_\chi(q) \bar{u}_\beta(q) \gamma^5 \gamma^\alpha U^\beta(p') \bar{U}_\mu(p') \varepsilon_\zeta(p) \varepsilon^{*\alpha}(p)}{(m_{P_D}^2 - p'^2) (m_{J/\psi}^2 - p^2) (m_\Delta^2 - q^2)} + \dots, \quad (32)$$

$$\Pi_{\mu\nu,9}(p, q) = \frac{\sqrt{2} f_{\eta_c} m_{\eta_c}^2}{2m_c} \lambda_N \lambda_{P_E} g_{\eta_c N,9} \frac{-i u(q) \bar{u}(q) U_{\alpha\beta}(p') \bar{U}_{\mu\nu}(p') p^\alpha p^\beta}{(m_{P_E}^2 - p'^2) (m_{\eta_c}^2 - p^2) (m_N^2 - q^2)} + \dots, \quad (33)$$

$$\Pi_{\mu\nu\zeta,10}(p, q) = \sqrt{2} f_{J/\psi} m_{J/\psi} \lambda_N \lambda_{P_E} g_{J/\psi N,10} \cdot \frac{u(q) \bar{u}(q) \gamma^5 \gamma_\chi U_{\alpha\beta}(p') \bar{U}_{\mu\nu}(p') \varepsilon_\zeta(p) \varepsilon^{*\chi}(p) p^\alpha p^\beta}{(m_{P_E}^2 - p'^2) (m_{J/\psi}^2 - p^2) (m_N^2 - q^2)} + \dots, \quad (34)$$

$$\Pi_{\mu\nu\chi,11}(p, q) = \frac{\sqrt{2} f_{\eta_c} m_{\eta_c}^2}{2m_c} \lambda_\Delta \lambda_{P_F} g_{\eta_c \Delta,11} \frac{-i u_\chi(q) \bar{u}^\alpha(q) \gamma^5 U_{\alpha\beta}(p') \bar{U}_{\mu\nu}(p') p^\beta}{(m_{P_F}^2 - p'^2) (m_{\eta_c}^2 - p^2) (m_\Delta^2 - q^2)} + \dots, \quad (35)$$

$$\Pi_{\mu\nu\chi\zeta,12}(p, q) = \sqrt{2} f_{J/\psi} m_{J/\psi} \lambda_\Delta \lambda_{P_F} g_{J/\psi \Delta,12} \cdot \frac{u_\chi(q) \bar{u}^\alpha(q) \gamma_\theta U_{\xi\alpha}(p') \bar{U}_{\mu\nu}(p') \varepsilon_\zeta(p) \varepsilon^{*\theta}(p) p^\alpha}{(m_{P_F}^2 - p'^2) (m_{J/\psi}^2 - p^2) (m_\Delta^2 - q^2)} + \dots, \quad (36)$$

where  $u(q)$  is the Dirac spinor;  $u_\mu(q)$ ,  $U_\mu(p')$ , and  $U_{\mu\nu}(p')$  are the Rarita-Schwinger spinors; and  $\varepsilon_z$  represents the polarization vector of the  $J/\psi$ . They follow the equations:

$$\begin{aligned} \sum_s u(q)\bar{u}(q) &= \not{q} + m_N, \\ \sum_s u_\mu(q)\bar{u}_\nu(q) &= (\not{q} + m_\Delta) \left( -g_{\mu\nu} + \frac{\gamma_\mu\gamma_\nu}{3} + \frac{2q_\mu q_\nu}{3q^2} - \frac{q_\mu\gamma_\nu - q_\nu\gamma_\mu}{3\sqrt{q^2}} \right), \\ \sum_s U_\mu(p')\bar{U}_\nu(p') &= (\not{p}' + m_{P_{A/B/C/D}}) \left( -g_{\mu\nu} + \frac{\gamma_\mu\gamma_\nu}{3} + \frac{2p'_\mu p'_\nu}{3p'^2} - \frac{p'_\mu\gamma_\nu - p'_\nu\gamma_\mu}{3\sqrt{p'^2}} \right), \end{aligned} \quad (37)$$

$$\begin{aligned} \sum_s U_{\mu\nu}(p')\bar{U}_{\alpha\beta}(p') &= (\not{p}' + m_{P_{E/F}}) \left\{ \frac{\tilde{g}_{\mu\alpha}(p')\tilde{g}_{\nu\beta}(p') + \tilde{g}_{\mu\beta}(p')\tilde{g}_{\nu\alpha}(p')}{2} - \frac{\tilde{g}_{\mu\nu}(p')\tilde{g}_{\alpha\beta}(p')}{5} \right. \\ &\quad - \frac{1}{10} \left( \gamma_\mu\gamma_\alpha + \frac{\gamma_\mu p'_\alpha - \gamma_\alpha p'_\mu}{\sqrt{p'^2}} - \frac{p'_\mu p'_\alpha}{p'^2} \right) \tilde{g}_{\nu\beta}(p') - \frac{1}{10} \left( \gamma_\nu\gamma_\alpha + \frac{\gamma_\nu p'_\alpha - \gamma_\alpha p'_\nu}{\sqrt{p'^2}} - \frac{p'_\nu p'_\alpha}{p'^2} \right) \tilde{g}_{\mu\beta}(p') \\ &\quad \left. - \frac{1}{10} \left( \gamma_\mu\gamma_\beta + \frac{\gamma_\mu p'_\beta - \gamma_\beta p'_\mu}{\sqrt{p'^2}} - \frac{p'_\mu p'_\beta}{p'^2} \right) \tilde{g}_{\nu\alpha}(p') - \frac{1}{10} \left( \gamma_\nu\gamma_\beta + \frac{\gamma_\nu p'_\beta - \gamma_\beta p'_\nu}{\sqrt{p'^2}} - \frac{p'_\nu p'_\beta}{p'^2} \right) \tilde{g}_{\mu\alpha}(p') \right\} \end{aligned} \quad (38)$$

where  $\tilde{g}_{\mu\nu}(p') = g_{\mu\nu} - \frac{p'_\mu p'_\nu}{p'^2}$ ,  $\varepsilon_\mu(p)\varepsilon_\nu^*(p) = -\tilde{g}_{\mu\nu}(p)$ ,  $\lambda_N$  and  $\lambda_\Delta$  are the pole residues of the  $N$  and  $\Delta$  baryons, respectively,  $\lambda_{P_{A-F}}$  represents the pole residues of the states  $P_c(4380)$ ,  $P_c(4410)$ ,  $P_c(4440)$ ,  $P_c(4470)$ ,  $P_c(4457)$ , and  $P_c(4620)$ .  $f_{\eta_c}$  and  $f_{J/\psi}$  are the decay constants of the  $\eta_c$  and  $J/\psi$  mesons, respectively.  $g_{\eta_c N, 1/5/9}$  and  $g_{J/\psi N, 2/6/10}$  denote the strong decay constants for the decay channels  $\mathcal{P}_{A/C/E} \rightarrow \eta_c N$  and  $\mathcal{P}_{A/C/E} \rightarrow J/\psi N$  of the  $P_c(4380)$ ,  $P_c(4440)$ , and  $P_c(4457)$ , respectively.  $g_{\eta_c \Delta, 3/7/11}$  and  $g_{J/\psi \Delta, 4/8/12}$  are the strong decay constants for the decay channels  $\mathcal{P}_{B/D/F} \rightarrow \eta_c \Delta$  and  $\mathcal{P}_{B/D/F} \rightarrow J/\psi \Delta$  of the  $P_c(4410)$ ,  $P_c(4470)$ , and  $P_c(4620)$ , respectively. As shown,  $\mathcal{P}_{A-F}$  represent the above six  $P_c$  states. The listed constants are defined as follows:

$$\begin{aligned} \langle 0 | \mathcal{J}_N(0) | N(q) \rangle &= \lambda_N u(q), \\ \langle 0 | \mathcal{J}_{\Delta\mu}(0) | \Delta(q) \rangle &= \lambda_\Delta u_\mu(q), \\ \langle 0 | \mathcal{J}_{J/\psi, \mu}(0) | J/\psi(p) \rangle &= f_{J/\psi} m_{J/\psi} \varepsilon_\mu, \end{aligned} \quad (39)$$

$$\langle 0 | \mathcal{J}_{\eta_c}(0) | \eta_c(p) \rangle = \frac{f_{\eta_c} m_{\eta_c}^2}{2m_c},$$

$$\begin{aligned} \langle 0 | \mathcal{J}_{P_{A/B/C/D}, \mu}(0) | \mathcal{P}_{A/B/C/D}(p') \rangle &= \lambda_{P_{A/B/C/D}} U_\mu(p'), \\ \langle 0 | \mathcal{J}_{P_{E/F}, \mu\nu}(0) | \mathcal{P}_{E/F}(p') \rangle &= \sqrt{2} \lambda_{P_{E/F}} U_{\mu\nu}(p'), \end{aligned} \quad (40)$$

$$\begin{aligned} \langle \eta_c(p) N(q) | \mathcal{P}_A(p') \rangle &= i g_{\eta_c N, 1} \bar{u}(q) i \gamma_5 U_\alpha(p') p^\alpha, \\ \langle J/\psi(p) N(q) | \mathcal{P}_A(p') \rangle &= g_{J/\psi N, 2} \bar{u}(q) U_\alpha(p') \varepsilon^{*\alpha}(p), \end{aligned} \quad (41)$$

$$\begin{aligned} \langle \eta_c(p) \Delta(q) | \mathcal{P}_B(p') \rangle &= -i g_{\eta_c \Delta, 3} \bar{u}_\beta(q) U^\beta(p'), \\ \langle J/\psi(p) \Delta(q) | \mathcal{P}_B(p') \rangle &= i g_{J/\psi \Delta, 4} \bar{u}^\beta(q) \gamma_5 \gamma_\alpha U_\beta(p') \varepsilon^{*\alpha}(p), \end{aligned} \quad (42)$$

$$\begin{aligned} \langle \eta_c(p) N(q) | \mathcal{P}_C(p') \rangle &= i g_{\eta_c N, 5} \bar{u}(q) i \gamma_5 U_\alpha(p') p^\alpha, \\ \langle J/\psi(p) N(q) | \mathcal{P}_C(p') \rangle &= -i g_{J/\psi N, 6} \bar{u}(q) U_\alpha(p') \varepsilon^{*\alpha}(p), \end{aligned} \quad (43)$$

$$\begin{aligned} \langle \eta_c(p) \Delta(q) | \mathcal{P}_D(p') \rangle &= -i g_{\eta_c \Delta, 7} \bar{u}_\beta(q) U^\beta(p'), \\ \langle J/\psi(p) \Delta(q) | \mathcal{P}_D(p') \rangle &= i g_{J/\psi \Delta, 8} \bar{u}^\beta(q) \gamma_5 \gamma_\alpha U_\beta(p') \varepsilon^{*\alpha}(p), \end{aligned} \quad (44)$$

$$\begin{aligned} \langle \eta_c(p) N(q) | \mathcal{P}_E(p') \rangle &= g_{\eta_c N, 9} \bar{u}(q) U_{\alpha\beta}(p') p^\alpha p^\beta, \\ \langle J/\psi(p) N(q) | \mathcal{P}_E(p') \rangle &= g_{J/\psi N, 10} \bar{u}(q) i \gamma_5 \gamma_\chi U_{\alpha\beta}(p') p^\alpha p^\beta \varepsilon^{*\chi}(p), \end{aligned} \quad (45)$$

$$\begin{aligned} \langle \eta_c(p) \Delta(q) | \mathcal{P}_F(p') \rangle &= -i g_{\eta_c \Delta, 11} \bar{u}^\chi(q) i \gamma_5 U_{\chi\beta}(p') p^\beta, \\ \langle J/\psi(p) \Delta(q) | \mathcal{P}_F(p') \rangle &= i g_{J/\psi \Delta, 12} \bar{u}^\xi(q) \gamma_\theta U_{\xi\chi}(p') p^\chi \varepsilon^{*\theta}(p), \end{aligned} \quad (46)$$

where  $m_c$ ,  $m_{\eta_c}$ ,  $m_{J/\psi}$ ,  $m_N$ ,  $m_\Delta$ , and  $m_{P_{A-F}}$  are the masses of the charm quark,  $\eta_c$ ,  $J/\psi$ ,  $N$ ,  $\Delta$ , and  $\mathcal{P}_{A-F}$ , respectively. The states  $|\eta_c\rangle$ ,  $|J/\psi\rangle$ ,  $|N\rangle$ ,  $|\Delta\rangle$ , and  $|\mathcal{P}_{A-F}\rangle$  denote the ground states of  $\eta_c$ ,  $J/\psi$ ,  $N$ ,  $\Delta$ , and  $\mathcal{P}_{A-F}$ , respectively.

The correlation functions at both the hadronic and QCD sides are matrices with complicated structures in the Dirac spinor space. It is reasonable to consider that the two sides should match each other, namely,

$\Pi_H(p, q) = \Pi_{QCD}(p, q)$ . In the framework of the QCD sum rules, the decay constants should not depend on the detailed structures. For example, the same decay constants are derived via different structures in Ref. [4]. The equations  $Tr[\Pi_H(p, q) \cdot \Gamma] = Tr[\Pi_{QCD}(p, q) \cdot \Gamma]$  are applied to select the detailed structures, where  $\Gamma$  is some chosen  $\gamma$ -matrix in the Dirac spinor space. The selected structures for both the hadronic and QCD sides are expressed as follows:

$$\begin{aligned}
\Pi_{\mu,1}(p, q) \cdot i\gamma_5 \tilde{g}_{\mu\nu}(p') &= \Pi_1(p'^2, p^2, q^2) \not{p} \not{q}_\nu + \dots, \\
\Pi_{\mu\zeta,2}(p, q) \tilde{g}_{\mu\nu}(p') &= \Pi_2(p'^2, p^2, q^2) \not{p} \not{q}_\nu q_\zeta + \dots, \\
\Pi_{\mu\chi,3}(p, q) \tilde{g}_{\mu\nu}(p') &= \Pi_3(p'^2, p^2, q^2) \not{p} \not{q}_\nu q_\chi + \dots, \\
\Pi_{\mu\chi\zeta,4}(p, q) \tilde{g}_{\mu\nu}(p') &= \Pi_4(p'^2, p^2, q^2) \not{p} \not{q}_\nu g_{\zeta\chi} + \dots, \\
\Pi_{\mu,5}(p, q) \cdot i\gamma_5 \tilde{g}_{\mu\nu}(p') &= \Pi_5(p'^2, p^2, q^2) \not{p} \not{q}_\nu + \dots, \\
\Pi_{\mu\zeta,6}(p, q) \tilde{g}_{\mu\nu}(p') &= \Pi_6(p'^2, p^2, q^2) \not{p} \not{q}_\nu q_\zeta + \dots, \\
\Pi_{\mu\chi,7}(p, q) \tilde{g}_{\mu\nu}(p') &= \Pi_7(p'^2, p^2, q^2) \not{p} \not{q}_\nu q_\chi + \dots, \\
\Pi_{\mu\chi\zeta,8}(p, q) \tilde{g}_{\mu\nu}(p') &= \Pi_8(p'^2, p^2, q^2) \not{p} \not{q}_\nu g_{\zeta\chi} + \dots, \\
\Pi_{\mu\nu,9}(p, q) \tilde{g}_{\mu\rho}(p') \tilde{g}_{\nu\sigma}(p') &= \Pi_9(p'^2, p^2, q^2) \not{p} \not{q}_\rho \sigma + \dots, \\
\Pi_{\mu\nu\zeta,10}(p, q) \cdot \gamma_5 \tilde{g}_{\mu\rho}(p') \tilde{g}_{\nu\sigma}(p') &= \Pi_{10}(p'^2, p^2, q^2) \not{p} \not{q}_\rho g_{\sigma\zeta} + \dots, \\
\Pi_{\mu\nu\chi,11}(p, q) \cdot i\gamma_5 \tilde{g}_{\mu\rho}(p') \tilde{g}_{\nu\sigma}(p') &= \Pi_{11}(p'^2, p^2, q^2) \not{p} \not{q}_\rho q_\chi + \dots, \\
\Pi_{\mu\nu\chi\zeta,12}(p, q) \tilde{g}_{\mu\rho}(p') \tilde{g}_{\nu\sigma}(p') &= \Pi_{12}(p'^2, p^2, q^2) \not{p} \not{q}_\rho q_\zeta g_{\sigma\chi} + \dots.
\end{aligned} \tag{47}$$

For the  $J^P = \frac{5}{2}^-$ , the two-point correlation function determined by the current  $\mathcal{J}_{P_E, \mu\nu}(x)$  or  $\mathcal{J}_{P_F, \mu\nu}(x)$  on the hadron side can be written as follows [38]:

$$\begin{aligned}
\Pi_{\mu\nu\alpha\beta}(p') &= 2\lambda_{\frac{5}{2}}^{-2} \frac{h' + m_-}{m_-^2 - h'^2} \left[ \frac{\tilde{g}_{\mu\alpha} \tilde{g}_{\nu\beta} + \tilde{g}_{\mu\beta} \tilde{g}_{\nu\alpha}}{2} - \frac{\tilde{g}_{\mu\nu} \tilde{g}_{\alpha\beta}}{5} \right. \\
&\quad \left. - \frac{1}{10} \left( \gamma_\mu \gamma_\alpha + \frac{\gamma_\mu p'_\alpha - \gamma_\alpha p'_\mu}{\sqrt{p'^2}} - \frac{p'_\mu p'_\alpha}{p'^2} \right) \right]
\end{aligned}$$

$$\begin{aligned}
&\cdot \tilde{g}_{\nu\beta} - \frac{1}{10} \left( \gamma_\nu \gamma_\alpha + \frac{\gamma_\nu p'_\alpha - \gamma_\alpha p'_\nu}{\sqrt{p'^2}} - \frac{p'_\nu p'_\alpha}{p'^2} \right) \tilde{g}_{\mu\beta} + \dots \Big] \\
&+ f_{\frac{5}{2}}^{-2} \frac{h' - m_-}{m_-^2 - h'^2} \left[ p'_\mu p'_\alpha \left( -g_{\nu\beta} + \frac{\gamma_\nu \gamma_\beta}{3} + \frac{2p'_\nu p'_\beta}{3p'^2} \right. \right. \\
&\quad \left. \left. - \frac{p'_\nu \gamma_\beta - p'_\beta \gamma_\nu}{3\sqrt{p'^2}} \right) + \dots \right] + h_{\frac{5}{2}}^{-2} \frac{h' + m_-}{m_-^2 - h'^2} p'_\mu p'_\nu p'_\alpha p'_\beta + \dots, \tag{48}
\end{aligned}$$

where we have already selected the negative parity, the items containing the parameters  $f_{\frac{5}{2}}^-$  and  $h_{\frac{5}{2}}^-$  are the components coupling to angular momentum  $\frac{5}{2}$  and  $\frac{1}{2}$ , respectively. Obviously,  $\mathcal{F}_{\frac{5}{2}} p'_\mu p'_\alpha = 0$  and  $\mathcal{F}_{\frac{5}{2}} p'_\mu p'_\nu p'_\alpha p'_\beta = 0$ , where  $\mathcal{F}_{\frac{5}{2}} = \tilde{g}_{\mu\nu}(p') \tilde{g}_{\alpha\beta}(p')$  is the projector used to obtain the component of the correlation function with angular momentum  $J = \frac{5}{2}$ . One could easily find that the projector for  $J = \frac{3}{2}$  can be set as  $\mathcal{F}_{\frac{3}{2}} = \tilde{g}_{\mu\nu}(p')$ .

On the QCD side, the Wick theorem is applied, and the correlation functions are then expressed in terms of the full propagators. Followed by the operator product expansion, the traces are performed, and the selected tensor structures are chosen. Thus,  $\Pi_{1-12}(p'^2, p^2, q^2)$  are derived on the QCD side. Since  $p' = p + q$  for the strong decays, considering the expressions of the correlation functions for Eqs.(25-36) and taking Eq.(25) as an example, it is impossible to deal with the correlation function strictly with the denominator  $[m_{P_A}^2 - (p+q)^2] (m_{\eta_c}^2 - p^2) (m_N^2 - q^2)$ . A similar situation occurs for the correlation function on the QCD side.  $p'^2$  is approximately set as  $\xi p^2$ , where  $\xi$  is a parameter. One can show that  $0 \leq \xi \leq \frac{2q^2}{p^2} + 2$ . For the decay  $P_c(4380) \rightarrow \eta_c + N$ ,  $0 \leq \xi \leq \frac{2m_N^2}{m_{\eta_c}^2} + 2$ , and  $\xi$  is set as  $\frac{m_N^2}{m_{\eta_c}^2} + 1$ . Following our previous works [44, 47–52], rigorous quark-hadron duality below the continuum thresholds is assumed, and the double Borel transformation is performed. The QCD sum rules for the hadronic coupling constants are given by,

$$\begin{aligned}
&\frac{f_{\eta_c} m_{\eta_c}^2 \lambda_N \lambda_{P_A} g_{\eta_c N,1}}{2m_c \xi} \frac{\kappa_1}{\frac{m_{P_A}^2}{\xi} - m_{\eta_c}^2} \left\{ \exp\left(-\frac{m_{\eta_c}^2}{T_1^2}\right) - \exp\left(-\frac{m_{P_A}^2}{\xi T_1^2}\right) \right\} \exp\left(-\frac{m_N^2}{T_2^2}\right) + C_1 \exp\left(-\frac{m_{\eta_c}^2}{T_1^2} - \frac{m_N^2}{T_2^2}\right) \\
&= \int_{4m_c^2}^{s_{\eta_c}^0} ds \int_0^{s_N^0} du \rho_1(s, u) \exp\left(-\frac{s}{T_1^2} - \frac{u}{T_2^2}\right), \tag{49}
\end{aligned}$$

$$\begin{aligned}
&\frac{f_{J/\psi} m_{J/\psi} \lambda_N \lambda_{P_A} g_{J/\psi N,2}}{\xi} \frac{\kappa_2}{\frac{m_{P_A}^2}{\xi} - m_{J/\psi}^2} \left\{ \exp\left(-\frac{m_{J/\psi}^2}{T_1^2}\right) - \exp\left(-\frac{m_{P_A}^2}{\xi T_1^2}\right) \right\} \exp\left(-\frac{m_N^2}{T_2^2}\right) + C_2 \exp\left(-\frac{m_{J/\psi}^2}{T_1^2} - \frac{m_N^2}{T_2^2}\right)
\end{aligned}$$

$$= \int_{4m_c^2}^{s_{J/\psi}^0} ds \int_0^{s_N^0} du \rho_2(s, u) \exp\left(-\frac{s}{T_1^2} - \frac{u}{T_2^2}\right), \quad (50)$$

$$\frac{f_{\eta_c} m_{\eta_c}^2 \lambda_{\Delta} \lambda_{P_B} g_{\eta_c \Delta, 3}}{2m_c \xi} \frac{\kappa_3}{\frac{m_{P_B}^2}{\xi} - m_{\eta_c}^2} \left\{ \exp\left(-\frac{m_{\eta_c}^2}{T_1^2}\right) - \exp\left(-\frac{m_{P_B}^2}{\xi T_1^2}\right) \right\} \exp\left(-\frac{m_{\Delta}^2}{T_2^2}\right) + C_3 \exp\left(-\frac{m_{\eta_c}^2}{T_1^2} - \frac{m_{\Delta}^2}{T_2^2}\right)$$

$$= \int_{4m_c^2}^{s_{\eta_c}^0} ds \int_0^{s_{\Delta}^0} du \rho_3(s, u) \exp\left(-\frac{s}{T_1^2} - \frac{u}{T_2^2}\right), \quad (51)$$

$$\frac{f_{J/\psi} m_{J/\psi} \lambda_{\Delta} \lambda_{P_B} g_{J/\psi \Delta, 4}}{\xi} \frac{\kappa_4}{\frac{m_{P_B}^2}{\xi} - m_{J/\psi}^2} \left\{ \exp\left(-\frac{m_{J/\psi}^2}{T_1^2}\right) - \exp\left(-\frac{m_{P_B}^2}{\xi T_1^2}\right) \right\} \exp\left(-\frac{m_{\Delta}^2}{T_2^2}\right) + C_4 \exp\left(-\frac{m_{J/\psi}^2}{T_1^2} - \frac{m_{\Delta}^2}{T_2^2}\right)$$

$$= \int_{4m_c^2}^{s_{J/\psi}^0} ds \int_0^{s_{\Delta}^0} du \rho_4(s, u) \exp\left(-\frac{s}{T_1^2} - \frac{u}{T_2^2}\right), \quad (52)$$

$$\frac{f_{\eta_c} m_{\eta_c}^2 \lambda_N \lambda_{P_C} g_{\eta_c N, 5}}{2m_c \xi} \frac{\kappa_5}{\frac{m_{P_C}^2}{\xi} - m_{\eta_c}^2} \left\{ \exp\left(-\frac{m_{\eta_c}^2}{T_1^2}\right) - \exp\left(-\frac{m_{P_C}^2}{\xi T_1^2}\right) \right\} \exp\left(-\frac{m_N^2}{T_2^2}\right) + C_5 \exp\left(-\frac{m_{\eta_c}^2}{T_1^2} - \frac{m_N^2}{T_2^2}\right)$$

$$= \int_{4m_c^2}^{s_{\eta_c}^0} ds \int_0^{s_N^0} du \rho_5(s, u) \exp\left(-\frac{s}{T_1^2} - \frac{u}{T_2^2}\right), \quad (53)$$

$$\frac{f_{J/\psi} m_{J/\psi} \lambda_N \lambda_{P_C} g_{J/\psi N, 6}}{\xi} \frac{\kappa_6}{\frac{m_{P_C}^2}{\xi} - m_{J/\psi}^2} \left\{ \exp\left(-\frac{m_{J/\psi}^2}{T_1^2}\right) - \exp\left(-\frac{m_{P_C}^2}{\xi T_1^2}\right) \right\} \exp\left(-\frac{m_N^2}{T_2^2}\right) + C_6 \exp\left(-\frac{m_{J/\psi}^2}{T_1^2} - \frac{m_N^2}{T_2^2}\right)$$

$$= \int_{4m_c^2}^{s_{J/\psi}^0} ds \int_0^{s_N^0} du \rho_6(s, u) \exp\left(-\frac{s}{T_1^2} - \frac{u}{T_2^2}\right), \quad (54)$$

$$\frac{f_{\eta_c} m_{\eta_c}^2 \lambda_{\Delta} \lambda_{P_D} g_{\eta_c \Delta, 7}}{2m_c \xi} \frac{\kappa_7}{\frac{m_{P_D}^2}{\xi} - m_{\eta_c}^2} \left\{ \exp\left(-\frac{m_{\eta_c}^2}{T_1^2}\right) - \exp\left(-\frac{m_{P_D}^2}{\xi T_1^2}\right) \right\} \exp\left(-\frac{m_{\Delta}^2}{T_2^2}\right) + C_7 \exp\left(-\frac{m_{\eta_c}^2}{T_1^2} - \frac{m_{\Delta}^2}{T_2^2}\right)$$

$$= \int_{4m_c^2}^{s_{\eta_c}^0} ds \int_0^{s_{\Delta}^0} du \rho_7(s, u) \exp\left(-\frac{s}{T_1^2} - \frac{u}{T_2^2}\right), \quad (55)$$

$$\frac{f_{J/\psi} m_{J/\psi} \lambda_{\Delta} \lambda_{P_D} g_{J/\psi \Delta, 8}}{\xi} \frac{\kappa_8}{\frac{m_{P_D}^2}{\xi} - m_{J/\psi}^2} \left\{ \exp\left(-\frac{m_{J/\psi}^2}{T_1^2}\right) - \exp\left(-\frac{m_{P_D}^2}{\xi T_1^2}\right) \right\} \exp\left(-\frac{m_{\Delta}^2}{T_2^2}\right) + C_8 \exp\left(-\frac{m_{J/\psi}^2}{T_1^2} - \frac{m_{\Delta}^2}{T_2^2}\right)$$

$$= \int_{4m_c^2}^{s_{J/\psi}^0} ds \int_0^{s_{\Delta}^0} du \rho_8(s, u) \exp\left(-\frac{s}{T_1^2} - \frac{u}{T_2^2}\right), \quad (56)$$

$$\begin{aligned} & \frac{f_{\eta_c} m_{\eta_c}^2 \lambda_N \lambda_{P_E} g_{\eta_c N,9}}{2m_c \xi} \frac{\sqrt{2}\kappa_9}{\frac{m_{P_E}^2}{\xi} - m_{\eta_c}^2} \left\{ \exp\left(-\frac{m_{\eta_c}^2}{T_1^2}\right) - \exp\left(-\frac{m_{P_E}^2}{\xi T_1^2}\right) \right\} \exp\left(-\frac{m_N^2}{T_2^2}\right) + C_9 \exp\left(-\frac{m_{\eta_c}^2}{T_1^2} - \frac{m_N^2}{T_2^2}\right) \\ &= \int_{4m_c^2}^{s_{\eta_c}^0} ds \int_0^{s_N^0} du \rho_9(s, u) \exp\left(-\frac{s}{T_1^2} - \frac{u}{T_2^2}\right), \end{aligned} \quad (57)$$

$$\begin{aligned} & \frac{f_{J/\psi} m_{J/\psi} \lambda_N \lambda_{P_E} g_{J/\psi N,10}}{\xi} \frac{\sqrt{2}\kappa_{10}}{\frac{m_{P_E}^2}{\xi} - m_{J/\psi}^2} \left\{ \exp\left(-\frac{m_{J/\psi}^2}{T_1^2}\right) - \exp\left(-\frac{m_{P_E}^2}{\xi T_1^2}\right) \right\} \exp\left(-\frac{m_N^2}{T_2^2}\right) + C_{10} \exp\left(-\frac{m_{J/\psi}^2}{T_1^2} - \frac{m_N^2}{T_2^2}\right) \\ &= \int_{4m_c^2}^{s_{J/\psi}^0} ds \int_0^{s_N^0} du \rho_{10}(s, u) \exp\left(-\frac{s}{T_1^2} - \frac{u}{T_2^2}\right), \end{aligned} \quad (58)$$

$$\begin{aligned} & \frac{f_{\eta_c} m_{\eta_c}^2 \lambda_{\Delta} \lambda_{P_F} g_{\eta_c \Delta,11}}{2m_c \xi} \frac{\sqrt{2}\kappa_{11}}{\frac{m_{P_F}^2}{\xi} - m_{\eta_c}^2} \left\{ \exp\left(-\frac{m_{\eta_c}^2}{T_1^2}\right) - \exp\left(-\frac{m_{P_F}^2}{\xi T_1^2}\right) \right\} \exp\left(-\frac{m_{\Delta}^2}{T_2^2}\right) + C_{11} \exp\left(-\frac{m_{\eta_c}^2}{T_1^2} - \frac{m_{\Delta}^2}{T_2^2}\right) \\ &= \int_{4m_c^2}^{s_{\eta_c}^0} ds \int_0^{s_{\Delta}^0} du \rho_{11}(s, u) \exp\left(-\frac{s}{T_1^2} - \frac{u}{T_2^2}\right), \end{aligned} \quad (59)$$

$$\begin{aligned} & \frac{f_{J/\psi} m_{J/\psi} \lambda_{\Delta} \lambda_{P_F} g_{J/\psi \Delta,12}}{\xi} \frac{\sqrt{2}\kappa_{12}}{\frac{m_{P_F}^2}{\xi} - m_{J/\psi}^2} \left\{ \exp\left(-\frac{m_{J/\psi}^2}{T_1^2}\right) - \exp\left(-\frac{m_{P_F}^2}{\xi T_1^2}\right) \right\} \exp\left(-\frac{m_{\Delta}^2}{T_2^2}\right) + C_{12} \exp\left(-\frac{m_{J/\psi}^2}{T_1^2} - \frac{m_{\Delta}^2}{T_2^2}\right) \\ &= \int_{4m_c^2}^{s_{J/\psi}^0} ds \int_0^{s_{\Delta}^0} du \rho_{12}(s, u) \exp\left(-\frac{s}{T_1^2} - \frac{u}{T_2^2}\right), \end{aligned} \quad (60)$$

where,

$$\begin{aligned} \kappa_1 &= \frac{m_N m_{P_A} [4(m_{\eta_c}^2 \tau - m_N^2) + 8m_{\eta_c}^2]}{3m_{\eta_c}^2 \xi} \\ &\quad - \frac{(m_{\eta_c}^2 \tau + m_N^2)[2(m_{\eta_c}^2 \tau - m_N^2) + 4m_{\eta_c}^2]}{3m_{\eta_c}^2 \xi} \end{aligned} \quad (61)$$

and

$$\rho_Z(s, u) = \lim_{\epsilon_2 \rightarrow 0} \lim_{\epsilon_1 \rightarrow 0} \frac{\text{Im}_s \text{Im}_u \Pi_Z(p'^2, s + i\epsilon_2, u + i\epsilon_1)}{\pi^2}, \quad (62)$$

The spectral densities at the QCD sides,  $\Pi_Z$ , are the correlation functions at the QCD sides selected from the corresponding structures in the same manner as the hadronic sides, where  $Z = 1 \sim 12$ . The parameters  $\kappa_{2\sim 12}$  are listed in the Appendix, while the complex expressions of the spectral densities at the QCD sides are omitted. The  $C_{1\sim 12}$  represent unknown parameters determined through numerical calculations to achieve flat platforms [44, 47–52]. To illustrate the origin of these free parameters, we consider

the decay channel  $P_c(4380) \rightarrow \eta_c + N$  as an example. By applying the triple dispersion relation, the correlation function  $\Pi_{\mu,1}$  at the hadronic side is expressed as follows:

$$\begin{aligned} & \Pi_{\mu,1,H}(p'^2, p^2, q^2) \\ &= \int_{\Delta_s^2}^{\infty} ds' \int_{\Delta_s^2}^{\infty} ds \int_{\Delta_u^2}^{\infty} du \frac{\rho_H(s', s, u)}{(s' - p'^2)(s - p^2)(u - q^2)}, \end{aligned} \quad (63)$$

where  $\Delta_s^2$ ,  $\Delta_s^2$ , and  $\Delta_u^2$  are thresholds. We introduce the subscript  $H$  to denote the hadron side. On the QCD side, the double dispersion relation is applied to acquire,

$$\Pi_{QCD}(p'^2, p^2, q^2) = \int_{\Delta_s^2}^{\infty} ds \int_{\Delta_u^2}^{\infty} du \frac{\rho_{QCD}(p'^2, s, u)}{(s - p^2)(u - q^2)}, \quad (64)$$

as

$$\lim_{\epsilon \rightarrow 0} \frac{\text{Im} \Pi_{QCD}(s' + i\epsilon, p^2, q^2)}{\pi} = 0. \quad (65)$$

Obviously, the triple dispersion relation on the hadron

side cannot match with the double dispersion relation on the QCD side. The integral over  $ds'$  is carried out first, and then the hadron side is matched with the QCD side below the continuum thresholds to acquire rigorous quark-hadron duality [47, 48].

$$\int_{\Delta_s^2}^{s_0} ds \int_{\Delta_u^2}^{u_0} du \frac{\rho_{QCD}(p'^2, s, u)}{(s-p^2)(u-q^2)} = \int_{\Delta_s^2}^{s_0} ds \int_{\Delta_u^2}^{u_0} du \left[ \int_{\Delta_s^2}^{\infty} ds' \frac{\rho_H(s', s, u)}{(s'-p'^2)(s-p^2)(u-q^2)} \right], \quad (66)$$

where  $s_0$  and  $u_0$  are the continuum thresholds. Then, the free parameter  $C_1$  is introduced to parameterize the contributions of transitions between the higher resonances (continuum states) in the  $s'$  channel and the ground state conventional meson-baryon pair. It is written as,

$$C_1 = \int_{s'_0}^{\infty} ds' \frac{\rho_H(s', m_{\eta_c}^2, m_N^2)}{(s' - m_{P_A}^2)(p^2 - m_{\eta_c}^2)(q^2 - m_N^2)}, \quad (67)$$

where  $s'_0$  is the continuum threshold parameter for the ground state,  $\rho_H(s', m_{\eta_c}^2, m_N^2)$  is the formal hadronic spectral density for transitions between the higher resonances (continuum states) in the  $s'$  channel and the ground state of the meson-baryon pair  $\eta_c N$ . For the hadron side and QCD side of the spectral density below the continuum thresholds  $s_0$  and  $u_0$  in the  $s$  and  $u$  channels, there is a one-to-one correspondence, while in the  $s'$  channel, there is no corresponding counterpart on the QCD side. Experimentally, the spectroscopy of the hidden-charm pentaquark states has not been established yet, making it impossible to determine its explicit expression at this point. It is reasonable to introduce a free parameter  $C_1$  to parameterize the contributions involving the higher resonances (continuum states) in the  $s'$  channel, which results in model dependence. At present, we have no choice but to accept this model dependence, and this is also why we set its uncertainty  $\delta C_1$  to zero. The correctness of this approach depends on further experimental progress. For more detailed discussions, one can consult Sect.7 in Ref.[38].

### III. NUMERICAL RESULTS AND DISCUSSIONS

Based on the detailed expressions of  $\rho_{1-12}$ , the numerical calculation is conducted. As for the vacuum condensates on the QCD side, the standard values are applied, which are listed as  $\langle \bar{q}q \rangle = -(0.24 \pm 0.01 \text{ GeV})^3$ ,  $\langle \bar{q}g_s \sigma Gq \rangle = m_0^2 \langle \bar{q}q \rangle$ ,  $m_0^2 = (0.8 \pm 0.1) \text{ GeV}^2$ ,  $\langle \frac{\alpha_s}{\pi} GG \rangle = (0.33 \text{ GeV})^4$  at the energy scale  $\mu = 1 \text{ GeV}$  [53–56], and the value of the  $\overline{MS}$  mass  $m_c(m_c) = 1.275 \pm 0.025 \text{ GeV}$  is applied from the Particle Data Group [57]. The energy-scale dependence

of these parameters is written as follows:

$$\langle \bar{q}q \rangle(\mu) = \langle \bar{q}q \rangle(1 \text{ GeV}) \left[ \frac{\alpha_s(1 \text{ GeV})}{\alpha_s(\mu)} \right]^{\frac{12}{33-2n_f}},$$

$$\langle \bar{q}g_s \sigma Gq \rangle(\mu) = \langle \bar{q}g_s \sigma Gq \rangle(1 \text{ GeV}) \left[ \frac{\alpha_s(1 \text{ GeV})}{\alpha_s(\mu)} \right]^{\frac{2}{33-2n_f}},$$

$$m_c(\mu) = m_c(m_c) \left[ \frac{\alpha_s(\mu)}{\alpha_s(m_c)} \right]^{\frac{12}{33-2n_f}},$$

$$\alpha_s(\mu) = \frac{1}{b_0 t} \left[ 1 - \frac{b_1}{b_0^2} \frac{\text{log}t}{t} + \frac{b_1^2 (\text{log}^2 t - \text{log}t - 1) + b_0 b_2}{b_0^4 t^2} \right],$$

$$\text{where } t = \log \frac{\mu^2}{\Lambda_{QCD}^2}, \quad b_0 = \frac{33-2n_f}{12\pi}, \quad b_1 = \frac{153-19n_f}{24\pi^2},$$

$$b_2 = \frac{2857 - \frac{5033}{9}n_f + \frac{325}{27}n_f^2}{128\pi^3}, \quad \text{and } \Lambda_{QCD} = 213 \text{ MeV}, 296$$

MeV, 339 MeV for the flavors  $n_f = 5, 4, 3$ , respectively [57, 58], and  $n_f = 4$  for the strong decays of the present study. For decay products containing  $\eta_c(J/\psi)$ , the energy scale  $\mu = \frac{1}{2}m_{\eta_c}(\frac{1}{2}m_{J/\psi})$ , respectively [44, 59].

The masses of the states  $\mathcal{P}_A$ ,  $\mathcal{P}_C$ , and  $\mathcal{P}_E$  obey the experimental data, set  $m_{P_A} = 4.380 \text{ GeV}$ ,  $m_{P_C} = 4.410 \text{ GeV}$ , and  $m_{P_E} = 4.457 \text{ GeV}$  [2]. The masses of the states  $\mathcal{P}_B$ ,  $\mathcal{P}_D$ , and  $\mathcal{P}_F$  follow our conclusion in Ref. [39], and set  $m_{P_B} = 4.410 \text{ GeV}$ ,  $m_{P_D} = 4.470 \text{ GeV}$ , and  $m_{P_F} = 4.620 \text{ GeV}$ . The masses of  $\eta_c$ ,  $J/\psi$ ,  $N$ , and  $\Delta$  are from the Particle Data Group [57], taking  $m_{\eta_c} = 2.984 \text{ GeV}$ ,  $m_{J/\psi} = 3.097 \text{ GeV}$ ,  $m_N = 0.938 \text{ GeV}$ , and  $m_\Delta = 1.232 \text{ GeV}$ . The values of the decay constants of the  $\eta_c$  and  $J/\psi$  follow the results in Ref. [60], choosing  $f_{J/\psi} = 0.418 \text{ GeV}$ ,  $f_{\eta_c} = 0.387 \text{ GeV}$ . For the pole residues,  $\lambda_N = 3.20 \times 10^{-2} \text{ GeV}^3$  [61],  $\lambda_\Delta = 7.63 \times 10^{-3} \text{ GeV}^3$  [4],  $\lambda_{P_A} = 1.97 \times 10^{-3} \text{ GeV}^6$ ,  $\lambda_{P_B} = 1.24 \times 10^{-3} \text{ GeV}^6$ ,  $\lambda_{P_C} = 3.60 \times 10^{-3} \text{ GeV}^6$ ,  $\lambda_{P_D} = 2.31 \times 10^{-3} \text{ GeV}^6$ ,  $\lambda_{P_E} = 4.05 \times 10^{-3} \text{ GeV}^6$ ,  $\lambda_{P_F} = 2.40 \times 10^{-3} \text{ GeV}^6$  [39]. For the threshold parameters, they are set as  $\sqrt{s_{\eta_c}^0} = 3.50 \text{ GeV}$ ,  $\sqrt{s_N^0} = 1.30 \text{ GeV}$ ,  $\sqrt{s_{J/\psi}^0} = 3.60 \text{ GeV}$  [44], and  $\sqrt{s_\Delta^0} = 1.61 \text{ GeV}$  [4].

Until now, the strong decay constants could be numerically solved as  $g_{\mathcal{Y}} = g_{\mathcal{Y}}(T_1^2, T_2^2)$ , which rely on the corresponding free parameters  $C_{1-12}$ , where  $\mathcal{Y}$  represents the twelve different decay constants. One could determine the free parameters via the "flat surfaces" of  $g_{\mathcal{Y}}(T_1^2, T_2^2)$  among the Borel windows [4]. As analyzed, it is straightforward to set  $T_1^2 = T_2^2 = T^2$  for simplicity [44, 51, 52, 62]. Furthermore, the Borel platforms of each coupling constant are determined under the same intervals of the Borel parameters  $T^2$ , setting  $(T^2)_{\max} - (T^2)_{\min} = 1 \text{ GeV}^2$ . The free parameters are listed as follows:

$$\begin{aligned}
C_1 &= (-2.5140 \times 10^{-4} + 1.0559 \times 10^{-5} T^2) \text{ GeV}^{10}, \\
C_2 &= (-1.6400 \times 10^{-4} + 5.0840 \times 10^{-7} T^2) \text{ GeV}^9, \\
C_3 &= (-2.4000 \times 10^{-4} - 2.2080 \times 10^{-6} T^2) \text{ GeV}^9, \\
C_4 &= (1.3250 \times 10^{-6} + 1.0998 \times 10^{-7} T^2 + 3.5113 \times 10^{-8} T^4) \text{ GeV}^{10}, \\
C_5 &= (-3.6080 \times 10^{-4} - 2.4174 \times 10^{-6} T^2) \text{ GeV}^{10}, \\
C_6 &= (-6.3488 \times 10^{-6} + 4.1775 \times 10^{-7} T^2) \text{ GeV}^9, \\
C_7 &= (-3.6960 \times 10^{-4} - 3.3264 \times 10^{-6} T^2 + 1.0349 \times 10^{-7} T^4) \text{ GeV}^9, \\
C_8 &= (-5.3440 \times 10^{-4} + 8.7642 \times 10^{-6} T^2 - 4.1790 \times 10^{-7} T^4) \text{ GeV}^{10}, \\
C_9 &= (-5.0000 \times 10^{-6} + 2.5000 \times 10^{-6} T^2 + 4.0000 \times 10^{-7} T^4) \text{ GeV}^{11}, \\
C_{10} &= (2.0000 \times 10^{-4} - 3.4000 \times 10^{-6} T^2) \text{ GeV}^{10}, \\
C_{11} &= (-3.5405 \times 10^{-6} + 1.4516 \times 10^{-7} T^2 - 3.8946 \times 10^{-8} T^4) \text{ GeV}^{10}, \\
C_{12} &= (-1.2240 \times 10^{-4} - 7.3440 \times 10^{-7} T^2 + 3.4272 \times 10^{-8} T^4) \text{ GeV}^9,
\end{aligned}$$

where  $T$  in the above expressions of  $C_{1\sim 12}$  have no units. Considering the numerous input parameters for the numerical calculation of the strong decay constants, their error bounds are somewhat complicated. The approximations  $\frac{\delta\lambda_P}{\lambda_P} = \frac{\delta\lambda_{P'}}{\lambda_{P'}} = \frac{\delta\lambda_\Delta}{\lambda_\Delta} = \frac{\delta\lambda_N}{\lambda_N} = \frac{\delta f_{J/\psi}}{f_{J/\psi}} = \frac{\delta f_{\eta_c}}{f_{\eta_c}}$  are used to estimate the uncertainties [52, 62], and the uncertainties of the  $m_{P_{A\sim F}}$  are neglected to avoid over-evaluation. Furthermore, the error bounds due to the uncertainties of the free parameters  $\delta C_{1\sim 12}$  are disregarded [44, 51, 52, 62]. For instance, in the QCD sum rules of Eq.(49), the uncertainty of the decay constant satisfies,

$$\begin{aligned}
& \frac{f_{\eta_c} m_{\eta_c}^2 \lambda_N \lambda_{P_A} g_{\eta_c N,1}}{2m_c \xi} \frac{\kappa_1}{\frac{m_{P_A}^2}{\xi} - m_{\eta_c}^2} \\
& \left\{ \exp\left(-\frac{m_{\eta_c}^2}{T_1^2}\right) - \exp\left(-\frac{m_{P_A}^2}{\xi T_1^2}\right) \right\} \exp\left(-\frac{m_N^2}{T_2^2}\right) \\
& \cdot \left( \frac{\delta f_{\eta_c}}{f_{\eta_c}} + \frac{\delta\lambda_N}{\lambda_N} + \frac{\delta\lambda_{P_A}}{\lambda_{P_A}} + \frac{\delta g_{\eta_c N,1}}{g_{\eta_c N,1}} \right) \\
& = \delta \int_{4m_c^2}^{s_0} ds \int_0^{s_N} du \rho_1(s, u) \exp\left(-\frac{s}{T_1^2} - \frac{u}{T_2^2}\right), \quad (68)
\end{aligned}$$

Until now, there is no perfect way to deal with complex items like  $\frac{\delta f_{\eta_c}}{f_{\eta_c}} + \frac{\delta\lambda_N}{\lambda_N} + \frac{\delta\lambda_{P_A}}{\lambda_{P_A}} + \frac{\delta g_{\eta_c N,1}}{g_{\eta_c N,1}}$ . To find a practical way to address the uncertainty of the strong decay constant strictly, the approximation  $\frac{\delta f_{\eta_c}}{f_{\eta_c}} = \frac{\delta\lambda_N}{\lambda_N} = \frac{\delta\lambda_{P_A}}{\lambda_{P_A}} = \frac{\delta g_{\eta_c N,1}}{g_{\eta_c N,1}}$  is applied. The uncertainty of  $g_{\eta_c N,1}$  is derived as follows:

$$\delta g_{\eta_c N,1} = \frac{1}{4} \sqrt{\sum_i [g_{\eta_c N,1}(x_i + \delta x_i) - g_{\eta_c N,1}(x_i)]^2},$$

where  $x_i$  are the input parameters due to the vacuum con-

densates  $\langle \bar{q}q \rangle$ ,  $\langle \bar{q}g_s \sigma Gq \rangle$ , and  $m_c(m_c)$ , and  $\delta x_i$  are their uncertainties. The reason for neglecting the uncertainties of masses such as  $m_{P_{A\sim F}}$ ,  $m_{\eta_c}$ , and so on, to avoid over-evaluation, is then obvious, since their uncertainties also stem from these input parameters  $x_i$  within the framework of QCD sum rules.

Accordingly, the graphs of the decay constants are shown in Figures 1 through 6, and the extracted values of the strong decay constants are listed in Table 1. The related decay widths are as follows:

$$\Gamma_{J,1\sim 12} = \sum_s |\mathcal{T}_{1\sim 12}^2| \frac{\mathcal{S}(m_{P_{A\sim F}}, m_1, m_2)}{8(2J+1)\pi m_{P_{A\sim F}}^2} \quad (69)$$

where  $J$  is the angular momentum of the states  $\mathcal{P}_{A\sim F}$ ,  $m_1$  and  $m_2$  are the masses of the decay products,  $\mathcal{S}(a, b, c) = \frac{\sqrt{a^2-(b+c)^2} \sqrt{a^2-(b-c)^2}}{2a}$ , and  $\mathcal{T}_{1\sim 12}$  are the decay vertices listed on the left sides of Eqs. [41-46]. Take the decay channel  $P_c(4380) \rightarrow \eta_c N$  for example, where  $m_1 = m_{\eta_c}$ ,  $m_2 = m_N$ ,  $J = \frac{3}{2}$ , and  $\mathcal{T}_1 = \langle \eta_c(p) N(q) | \mathcal{P}_A(p') \rangle$ . The decay widths  $\Gamma_{A\sim F}$  of the  $\mathcal{P}_{A\sim F}$  are determined as follows:

$$\begin{aligned}
\Gamma_A &= 158.86_{-6.82}^{+12.67} \text{ MeV}, \\
\Gamma_B &= 98.35_{-39.13}^{+39.13} \text{ MeV}, \\
\Gamma_C &= 17.37_{-3.68}^{+3.68} \text{ MeV}, \\
\Gamma_D &= 126.88_{-85.45}^{+123.76} \text{ MeV}, \\
\Gamma_E &= 5.63_{-0.85}^{+0.85} \text{ MeV}, \\
\Gamma_F &= 77.54_{-60.35}^{+64.10} \text{ MeV}.
\end{aligned}$$

The ratios of the partial decay widths of the  $\mathcal{P}_{A\sim F}$  are

$$\begin{aligned}
\frac{\Gamma[P_c(4380) \rightarrow \eta_c N]}{\Gamma[P_c(4380) \rightarrow J/\psi N]} &= 28.53, \\
\frac{\Gamma[P_c(4410) \rightarrow \eta_c \Delta]}{\Gamma[P_c(4410) \rightarrow J/\psi \Delta]} &= 1.30, \\
\frac{\Gamma[P_c(4440) \rightarrow \eta_c N]}{\Gamma[P_c(4440) \rightarrow J/\psi N]} &= 0.56, \\
\frac{\Gamma[P_c(4470) \rightarrow \eta_c \Delta]}{\Gamma[P_c(4470) \rightarrow J/\psi \Delta]} &= 0.68, \\
\frac{\Gamma[P_c(4457) \rightarrow \eta_c N]}{\Gamma[P_c(4457) \rightarrow J/\psi N]} &= 0.84, \\
\frac{\Gamma[P_c(4620) \rightarrow \eta_c \Delta]}{\Gamma[P_c(4620) \rightarrow J/\psi \Delta]} &= 0.29.
\end{aligned}$$

Results show that the decay widths of the discovered  $P_c(4380)$ ,  $P_c(4440)$ , and  $P_c(4457)$  are in good agreement with data proposed by the LHCb [1, 2]. Particularly, for the wide width  $P_c(4380)$  state, the main decay channel is  $P_c(4380) \rightarrow \eta_c N$ , which contributes nearly 97% of the

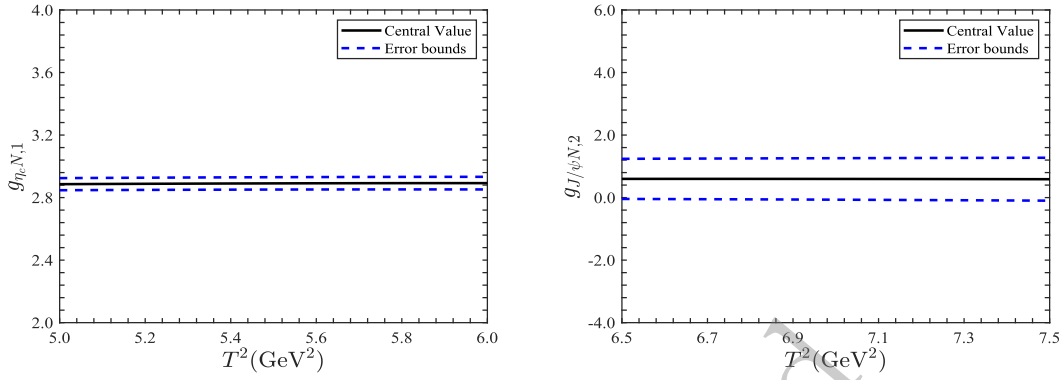


**Fig. 1.** (color online) The hadronic coupling constants for  $P_c(4380) \rightarrow \eta_c N$  (left) and  $P_c(4380) \rightarrow J/\psi N$  (right) within the Borel windows.

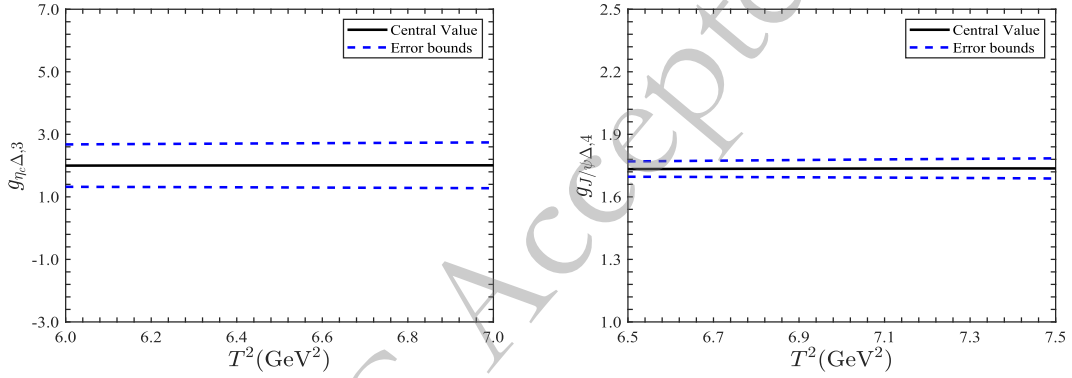


**Fig. 2.** (color online) The hadronic coupling constants for  $P_c(4410) \rightarrow \eta_c \Delta$  (left) and  $P_c(4410) \rightarrow J/\psi \Delta$  (right) among the Borel windows.

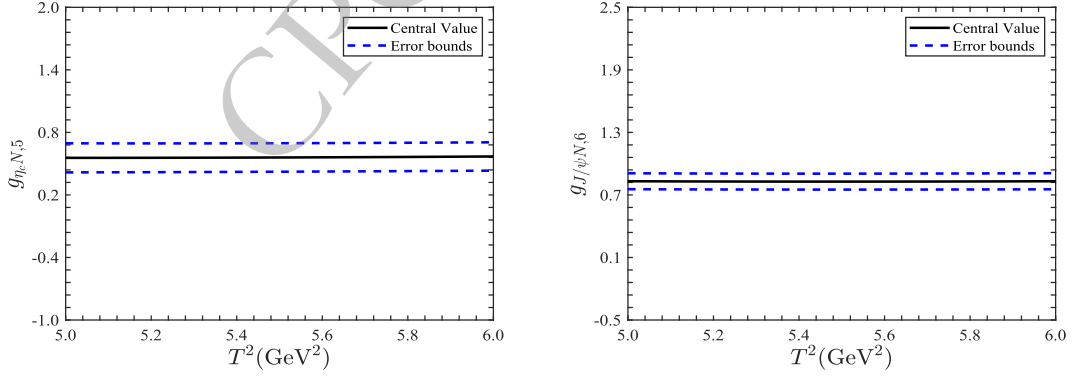


**Fig. 3.** (color online) The hadronic coupling constants for  $P_c(4440) \rightarrow \eta_c N$  (left) and  $P_c(4440) \rightarrow J/\psi N$  (right) among the Borel windows.

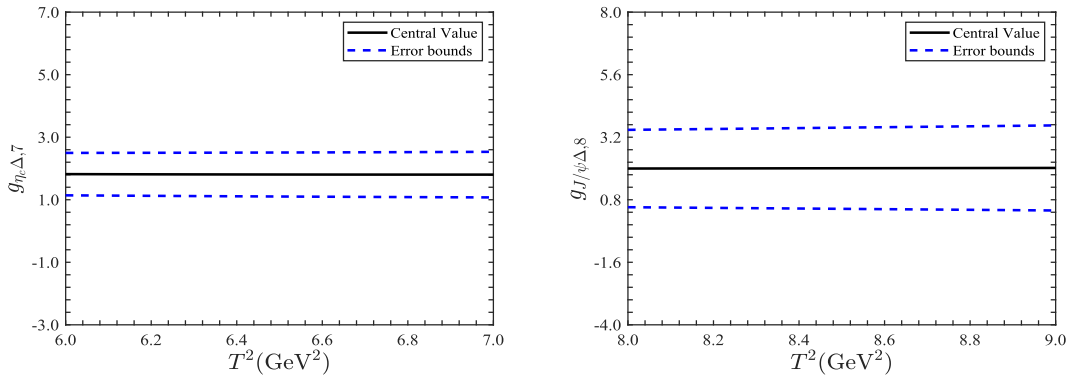


**Fig. 4.** (color online) The hadronic coupling constants for  $P_c(4470) \rightarrow \eta_c \Delta$  (left) and  $P_c(4470) \rightarrow J/\psi \Delta$  (right) among the Borel windows.

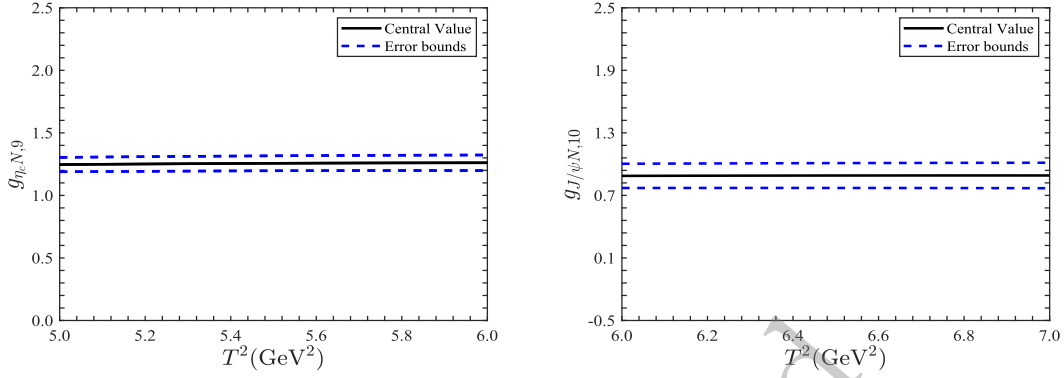


**Fig. 5.** (color online) The hadronic coupling constants for  $P_c(4457) \rightarrow \eta_c N$  (left) and  $P_c(4457) \rightarrow J/\psi N$  (right) among the Borel windows.

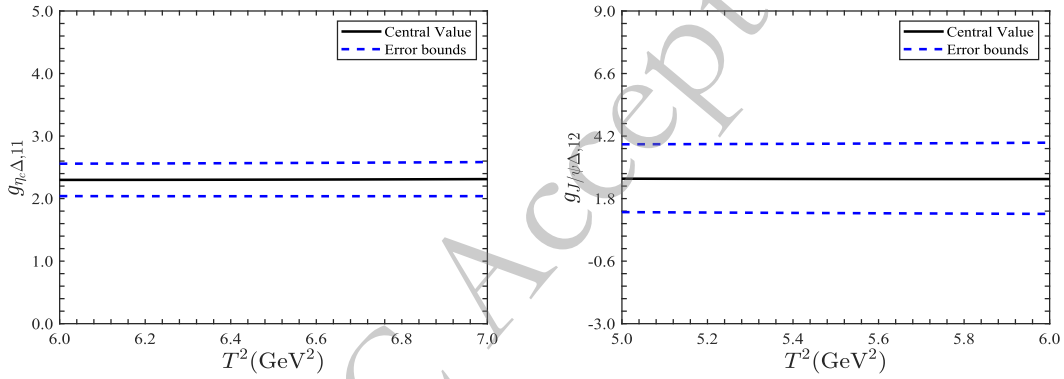


**Fig. 6.** (color online) The hadronic coupling constants for  $P_c(4620) \rightarrow \eta_c \Delta$  (left) and  $P_c(4620) \rightarrow J/\psi \Delta$  (right) among the Borel windows.

**Table 1.** Here is the revised text: The hadronic coupling constants extracted from the Borel windows and their corresponding decay widths are

$gZ$	$T^2$ (GeV <sup>2</sup> )	Values	Corresponding decay widths (MeV)
$g_{\eta_c N,1}$	5.0 – 6.0	$2.89^{+0.04}_{-0.04} \text{ GeV}^{-1}$	$153.48^{+4.19}_{-4.19}$
$g_{J/\psi N,2}$	6.5 – 7.5	$0.60^{+0.66}_{-0.60}$	$5.38^{+11.96}_{-5.38}$
$g_{\eta_c \Delta,3}$	6.0 – 7.0	$2.01^{+0.70}_{-0.70}$	$55.63^{+39.07}_{-39.07}$
$g_{J/\psi \Delta,4}$	6.5 – 7.5	$1.74^{+0.04}_{-0.04}$	$42.72^{+2.10}_{-2.10}$
$g_{\eta_c N,5}$	5.0 – 6.0	$0.56^{+0.14}_{-0.14} \text{ GeV}^{-1}$	$6.24^{+3.05}_{-3.05}$
$g_{J/\psi N,6}$	5.0 – 6.0	$0.83^{+0.08}_{-0.08}$	$11.13^{+2.06}_{-2.06}$
$g_{\eta_c \Delta,7}$	6.0 – 7.0	$1.81^{+0.70}_{-0.70}$	$51.37^{+40.00}_{-40.00}$
$g_{J/\psi \Delta,8}$	8.0 – 9.0	$2.01^{+1.56}_{-1.56}$	$75.51^{+117.12}_{-75.51}$
$g_{\eta_c N,9}$	5.0 – 6.0	$1.26^{+0.06}_{-0.06} \text{ GeV}^{-2}$	$2.57^{+0.24}_{-0.24}$
$g_{J/\psi N,10}$	6.0 – 7.0	$0.89^{+0.12}_{-0.12} \text{ GeV}^{-2}$	$3.06^{+0.82}_{-0.82}$
$g_{\eta_c \Delta,11}$	6.0 – 7.0	$2.30^{+0.27}_{-0.27} \text{ GeV}^{-1}$	$17.32^{+3.99}_{-3.99}$
$g_{J/\psi \Delta,12}$	5.0 – 6.0	$2.55^{+1.36}_{-1.31} \text{ GeV}^{-1}$	$60.22^{+63.98}_{-60.22}$

wide width  $158.86 \text{ MeV}$ , fitting the data  $205 \pm 18 \pm 86 \text{ MeV}$  observed by the LHCb.

The value of  $\zeta$  affects the correlation functions at both the hadronic and QCD sides, therefore impacting the choice of the related free parameter  $C$  and Borel platform.

As in our previous work's approximation model, we directly set  $p'^2 = p^2$ . Based on the range of  $\zeta$ ,  $0 \leq \zeta \leq \frac{2m_N^2}{m_{\eta_c}^2} + 2$ , and considering  $\frac{m_N^2}{m_{\eta_c}^2} \approx 0.1$ , for the decay channel  $P_c(4380) \rightarrow \eta_c + N$ , it is more reasonable to set

$\xi = \frac{m_N^2}{m_c^2} + 1$ . To evaluate the stability of the effect of  $\xi$ , we compare these two approximation models. As shown in Fig. 7, the value of the hadronic coupling constant extracted from the Borel window is  $g'_{\eta_c N,1} = 2.91^{+0.04}_{-0.04} \text{ GeV}^{-1}$  with  $\xi' = 1$  and the free parameter  $C'_1 = -2.7490 \times 10^{-4} + 1.0721 \times 10^{-5} T^2 \text{ GeV}^{10}$ . Results show that only a slight change occurs in the hadronic coupling constant, but the stability is robust.

Considering the two Borel parameters  $T_1^2$  and  $T_2^2$ , the chosen Borel platform should be a 'flat' plane [4]. Thus, any 'straight lines' on the plane are also flat, making it reasonable to set  $T_1^2 = T_2^2$  without significant change to the Borel window and the resulting value of the hadronic coupling constant. Of course, this may cause a slight difference. To discuss this clearly, we still take the decay channel  $P_c(4380) \rightarrow \eta_c + N$  as an example for comparison. In Fig. 8, the 3-D graph of the hadronic coupling constant  $g''_{\eta_c N,1}$  of the decay channel  $P_c(4380) \rightarrow \eta_c N$  across the Borel window is shown. The extracted value of the hadronic coupling constant is  $g''_{\eta_c N,1} = 2.87^{+0.05}_{-0.04} \text{ GeV}^{-1}$  with the free parameter  $C''_1 = -2.5000 \times 10^{-4} + 1.0250 \times 10^{-5} T_1^2 + 2.5000 \times 10^{-7} T_2^2 \text{ GeV}^{10}$ . The difference is acceptable.

It is important to point out that the chosen vacuum condensates are  $\langle \bar{q}q \rangle$ ,  $\langle \frac{\alpha_s}{\pi} GG \rangle$ ,  $\langle \bar{q}g_s \sigma Gq \rangle$ ,  $\langle \bar{q}q \rangle^2$ ,  $g_s^2 \langle \bar{q}q \rangle^2$ ,  $\langle \frac{\alpha_s}{\pi} GG \rangle \langle \bar{q}q \rangle$ ,  $\langle \bar{q}q \rangle \langle \bar{q}g_s \sigma Gq \rangle$ ,  $g_s^2 \langle \bar{q}q \rangle^3$ ,  $\langle \frac{\alpha_s}{\pi} GG \rangle \langle \bar{q}q \rangle^2$ , and  $\langle \bar{q}g_s \sigma Gq \rangle^2$  on the QCD sides. In the framework of QCD sum rules, these vacuum condensates are parameterized, and their values depend on the energy scale  $\mu$ , making the results in the present work have energy dependence. The decay products of all the decay channels studied are conventional hadrons. For the coupling of the QCD side and hadron side of the conventional hadron channel, there is no unified standard to determine the energy scale. It is reasonable to set the energy within an acceptable range. For example, we set the energy scale  $\mu = 1 \text{ GeV}$  to study the strong decay of hidden-charm tetraquark state candidates  $X(3872)$  and  $Y(4500)$  [64, 65]. In Refs. [4, 63], the energy scale is set as  $\frac{m_{\eta_c}}{2} \text{ GeV}$  or  $\frac{m_{J/\psi}}{2} \text{ GeV}$ , which is acceptable for charmonium states [59]. In Ref. [49], the energy scale is chosen as  $\mu = 2 \text{ GeV}$  to calculate the strong decay of  $X(4140)$  [49]. We plot the energy scale dependence of the vacuum condensates  $\langle \bar{q}q \rangle$  and  $\langle \bar{q}g_s \sigma Gq \rangle$  in Fig. 9. One can find that the value of these two vacuum condensates does not differ much with the energy scale varying from 1 GeV to 2 GeV; their tiny differences are less than their corresponding error bounds. The differences mainly occur for the strong fine-structure constant  $\alpha_s$  and  $m_c$ , with  $g_s^2 = 6.7381$  and  $3.6850$  at energy scales  $\mu = 1 \text{ GeV}$  and  $2 \text{ GeV}$ , respectively. The four-quark condensate  $g_s^2 \langle \bar{q}q \rangle^2$  arises from the terms  $\langle \bar{q} \gamma_\mu q g_s D_\eta G_{\lambda\tau} \rangle$ ,  $\langle \bar{q}_j D_\mu^\dagger D_\nu^\dagger D_\alpha^\dagger q_i \rangle$ , and  $\langle \bar{q}_j D_\mu D_\nu D_\alpha q_i \rangle$ , rather than from the radiative  $\mathcal{O}(\alpha_s)$  corrections for the four-quark condensate  $\langle \bar{q}q \rangle^2$ , where  $D_\alpha = \partial_\alpha - ig_s G_\alpha$ . The strong coupling con-

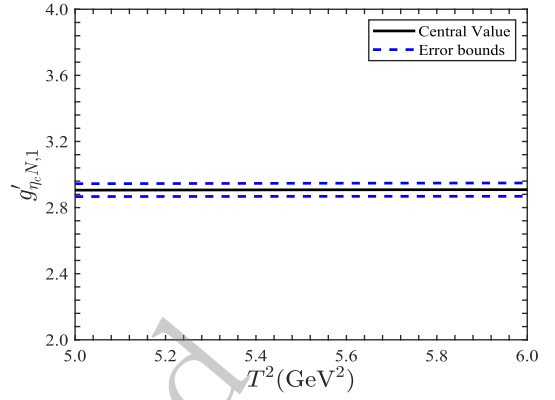


Fig. 7. (color online) The hadronic coupling constant  $g'_{\eta_c N,1}$  of the decay channel  $P_c(4380) \rightarrow \eta_c N$  is considered within the Borel window for the parameter  $\xi = 1$ .

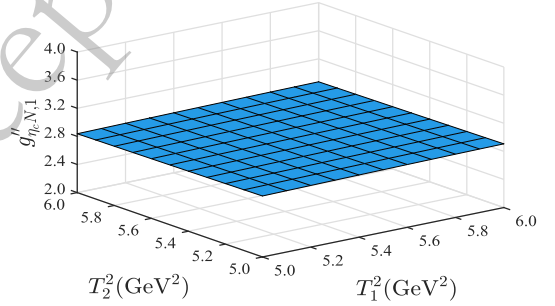


Fig. 8. (color online) The 3-D graph of the hadronic coupling constant  $g''_{\eta_c N,1}$  for the decay channel  $P_c(4380) \rightarrow \eta_c N$  within the Borel window is presented.

stant  $\alpha_s(\mu) = \frac{g_s^2(\mu)}{4\pi}$  appears at the tree level. In fact, the contributions of such terms are tiny. Thus, there is not much energy scale dependence for the contribution of the vacuum condensates. Taking the decay channel  $P_c(4380) \rightarrow \eta_c + N$  as an example, the energy scale dependence mainly arises from the following lower limit of the integral.

$$\int_{4m_c^2}^{s_{\eta_c}^0} ds \int_0^{s_N^0} du \rho_1(s, u) \exp\left(-\frac{s}{T_1^2} - \frac{u}{T_2^2}\right)$$

Since  $4m_c^2 = 8.8659 \text{ GeV}^2$  and  $4.9671 \text{ GeV}^2$  at the energy scale  $\mu = 1 \text{ GeV}$  and  $2 \text{ GeV}$ , respectively, in the present work, we follow our previous approach to set a medium energy scale,  $\mu = \frac{m_{\eta_c}}{2} \text{ GeV}$  or  $\mu = \frac{m_{J/\psi}}{2} \text{ GeV}$  [4, 63], to avoid a relatively large energy scale for the conventional hadron and to ensure the integral range maintains the stability of the Borel windows.

Before this study, several theoretical groups had proposed different physical models to study the strong decays of the discovered  $P_c$  states [19, 29, 30, 42–45, 66–71]. For example, Ref. [69] assigns the  $P_c(4440)$  and  $P_c(4457)$  as the  $\Sigma_c \bar{D}^*$  hadronic molecules with  $J^P$  being

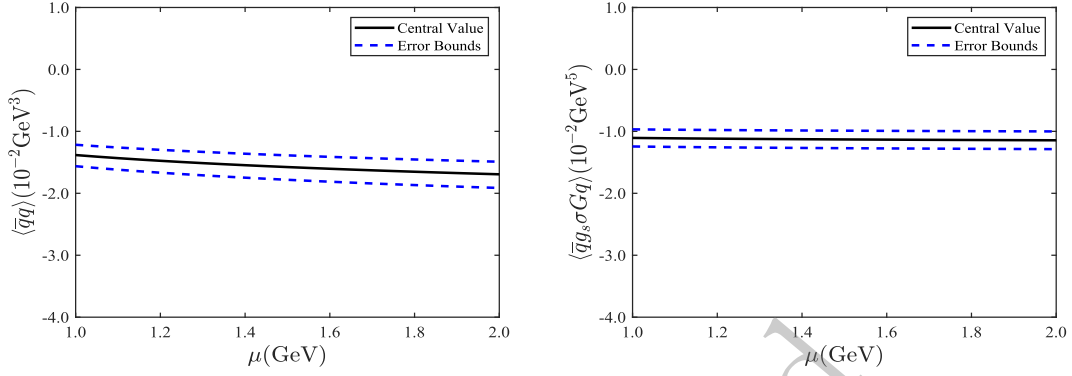


Fig. 9. (color online) The energy scale dependence of the vacuum condensates  $\langle \bar{q}q \rangle$  (left) and  $\langle \bar{q}g_s\sigma Gq \rangle$  (right).

$\frac{1^-}{2}$  or  $\frac{3^-}{2}$  via heavy quark spin symmetry (HQSS). For  $\frac{1^-}{2}$ ,  $\frac{\Gamma[P_c \rightarrow \eta_c p]}{\Gamma[P_c \rightarrow J/\psi p]} = \frac{3}{25}$ ; furthermore,  $\frac{\Gamma[P_c \rightarrow \Lambda_c \bar{D}^*]}{\Gamma[P_c \rightarrow \Lambda_c \bar{D}]} = \frac{4}{3}$ . By combining the effective Lagrangian and Bethe-Salpeter framework, Ref. [70] studied the strong decays of  $P_c(4440)$  and  $P_c(4457)$  for the decay channels  $\bar{D}^{(*)0}\Lambda_c^+$ ,  $J/\psi(\eta_c)p$ , and  $\bar{D}\Sigma_c^*$ , suggesting that the  $\bar{D}^0\Lambda_c$  and  $\bar{D}^{*0}\Lambda_c$  are the dominant decay channels for these two  $P_c$  states. Considering the compact pentaquark picture of the  $uudc\bar{c}$  pentaquark based on the flavor-spin model extended to  $SU(4)$ , Ref. [71] studied the ratios of decay rates of the  $P_c$  pentaquarks to  $J/\psi$  and similarly the ratios of decay rates  $\frac{\Gamma[P_c(\frac{1^-}{2}) \rightarrow \Lambda_c \bar{D}^*]}{\Gamma[P_c(\frac{1^-}{2}) \rightarrow \eta_c p]} = \frac{1}{3}$ . The fact is that there are varying arguments for the strong decays of these  $P_c$  states proposed by different theoretical groups. It is hard to determine which results have discriminating power among the different scenarios, including those predictions made in the present study. We noted the recent work of LHCb [72], where the collaboration performed a search for  $P_c(4312)$ ,  $P_c(4440)$ , and  $P_c(4457)$  states in the prompt  $\Sigma_c \bar{D}^{(*)}$ ,  $\Sigma_c^* \bar{D}^{(*)}$ ,  $\Lambda_c^+ \bar{D}^{(*)}$ , and  $\Lambda_c^+ \pi \bar{D}^{(*)}$  mass spectra. Their signal yields were found to be consistent with zero in all cases; thus, we follow these experimental results and study the present decay channels.

To date, we have systematically studied the hidden-charm pentaquark state candidates  $P_c(4312)$ ,  $P_c(4380)$ ,  $P_c(4440)$ , and  $P_c(4457)$ . In Ref. [39], the isospin is clearly differentiated for the first time under the framework of QCD sum rules. They are assigned as the  $\bar{D}\Sigma_c$ ,  $\bar{D}\Sigma_c^*$ ,  $\bar{D}^*\Sigma_c$ , and  $\bar{D}^*\Sigma_c^*$  molecular states with low isospin  $I = \frac{1}{2}$ , with their  $J^P$  being  $\frac{1^-}{2}$ ,  $\frac{3^-}{2}$ ,  $\frac{3^-}{2}$ , and  $\frac{5^-}{2}$ , respectively. Amid intense debates about the nature of these  $P_c$  states, we propose our own reasonable arguments. More significantly, high isospin  $I = \frac{3}{2}$  cousins  $P_c(4330)$ ,  $P_c(4410)$ ,  $P_c(4470)$ , and  $P_c(4620)$  are predicted. Results of the present work show that these high isospin cousins have

relatively wide widths, which are reasonable for assigning them as resonance states. The predictions for the high isospin cousins would provide an explicit reference for future experiments and will test our interpretation of the nature of the observed  $P_c(4312)$ ,  $P_c(4380)$ ,  $P_c(4440)$ , and  $P_c(4457)$  in return.

#### IV. CONCLUSIONS

In the present work, the strong decays of the exotic  $P_c(4380)$ ,  $P_c(4440)$ ,  $P_c(4457)$ , and their possible isospin cousins are studied. The decay channels of these  $P_c$  states,  $\mathcal{P}_{A \sim F} \rightarrow \eta_c(J/\psi) + N(\Delta)$ , are calculated via QCD sum rules. The decay widths of the  $P_c(4380)$ ,  $P_c(4440)$ , and  $P_c(4457)$  derived in this study are in good agreement with the experimental results observed by LHCb. The predicted strong decay widths for the  $P_c(4410)$ ,  $P_c(4470)$ , and  $P_c(4620)$  await verification in future experiments. Moreover, the ratios of the partial decay widths of these  $P_c$  states are determined. For example, it is found that the main decay channel for the  $P_c(4380)$  is  $P_c(4380) \rightarrow \eta_c N$ . These theoretical results may provide a reference for high-energy experiments. The strong decays of  $P_{cs}(4338)$  have been analyzed by our group [63], and the strong decays of  $P_{cs}(4459)$  and  $P_c(4337)$  will be our next target in the near future to provide a systematic picture of the strong decays of the pentaquark exotic  $P_c$  and  $P_{cs}$  states.

#### APPENDIX

$$\kappa_2 = \frac{4(m_{J/\psi}^2 \tau + m_N^2)}{3m_{J/\psi}^2 \xi} + \frac{8m_N m_{P_A}}{3m_{J/\psi}^2 \xi} \quad (\text{A1})$$

$$\begin{aligned} \kappa_3 = & -\frac{4m_{\eta_c}^2 \tau^2}{9m_{\Delta}^2 \xi} + \frac{4m_{\Delta}^2}{9m_{\eta_c}^2 \xi} + \frac{8m_{\eta_c}^2 \tau}{9m_{\Delta}^2} + \frac{4m_{\Delta} m_{P_B}}{3m_{\eta_c}^2 \xi} \\ & - \frac{4m_{\eta_c}^2 \xi}{9m_{\Delta} m_{P_B}} + \frac{4m_{\eta_c}^2 \tau}{9m_{\Delta} m_{P_B}} - \frac{4m_{P_B} \tau}{3m_{\Delta} \xi} + \frac{8m_{P_B}}{3m_{\Delta}} + \frac{16}{9} \end{aligned} \quad (\text{A2})$$

$$\kappa_4 = -\frac{8m_\Delta^2 m_{P_B}}{9m_{J/\psi}^2 \xi} + \frac{2m_\Delta^2}{9m_{P_B}} + \frac{2m_\Delta^3}{9m_{J/\psi}^2 \xi} + \frac{2m_{J/\psi}^2 \tau^2}{9m_\Delta \xi} - \frac{4m_{J/\psi}^2 \tau}{9m_\Delta} + \frac{4m_\Delta \tau}{9\xi} - \frac{4m_\Delta}{9} - \frac{4m_{J/\psi}^2 \xi}{9m_{P_B}} + \frac{2m_{J/\psi}^2 \tau}{9m_{P_B}} - \frac{8m_{P_B} \tau}{9\xi} + \frac{16m_{P_B}}{9} \quad (\text{A3})$$

$$\kappa_5 = \frac{4m_N^3 m_{P_C}}{3m_{\eta_c}^2 \xi} - \frac{2m_N^4}{3m_{\eta_c}^2 \xi} + \frac{4m_N^2}{3\xi} - \frac{4m_N m_{P_C} \tau}{3\xi} - \frac{8m_N m_{P_C}}{3\xi} + \frac{2m_{\eta_c}^2 \tau^2}{3\xi} + \frac{4m_{\eta_c}^2 \tau}{3\xi} \quad (\text{A4})$$

$$\kappa_6 = \frac{4m_N^2}{3m_{J/\psi}^2 \xi} + \frac{8m_N m_{P_C}}{3m_{J/\psi}^2 \xi} + \frac{4\tau}{3\xi} \quad (\text{A5})$$

$$\kappa_7 = \frac{4m_{\eta_c}^2 \tau^2}{9m_\Delta^2 \xi} - \frac{4m_\Delta^2}{9m_{\eta_c}^2 \xi} - \frac{8m_{\eta_c}^2 \tau}{9m_\Delta^2} - \frac{4m_\Delta m_{P_D}}{3m_{\eta_c}^2 \xi} + \frac{4m_{\eta_c}^2 \xi}{9m_\Delta m_{P_D}} - \frac{4m_{\eta_c}^2 \tau}{9m_\Delta m_{P_D}} + \frac{4m_{P_D} \tau}{3m_\Delta \xi} + \frac{8m_{P_D}}{3m_\Delta} - \frac{16}{9} \quad (\text{A6})$$

$$\kappa_8 = \frac{8m_\Delta^2 m_{P_D}}{9m_{J/\psi}^2 \xi} - \frac{2m_\Delta^2}{9m_{P_D}} - \frac{2m_\Delta^3}{9m_{J/\psi}^2 \xi} - \frac{2m_{J/\psi}^2 \tau^2}{9m_\Delta \xi} + \frac{4m_{J/\psi}^2 \tau}{9m_\Delta} - \frac{4m_\Delta \tau}{9\xi} + \frac{4m_\Delta}{9} + \frac{4m_{J/\psi}^2 \xi}{9m_{P_D}} - \frac{2m_{J/\psi}^2 \tau}{9m_{P_D}} + \frac{8m_{P_D} \tau}{9\xi} - \frac{16m_{P_D}}{9} \quad (\text{A7})$$

$$\kappa_9 = \frac{m_N^5 m_{P_E}}{5m_{\eta_c}^2 \xi} - \frac{2m_N^3 m_{P_E} \tau}{5\xi} - \frac{4m_N^3 m_{P_E}}{5\xi} - \frac{m_N^2 m_{\eta_c}^2 \tau^2}{10\xi} + \frac{m_N^6}{10m_{\eta_c}^2 \xi} + \frac{2m_N^2 m_{\eta_c}^2}{5\xi} - \frac{2m_N^2 m_{\eta_c}^2}{5} - \frac{m_N^4 \tau}{10\xi} - \frac{2m_N^4}{5\xi} \\ + \frac{m_N m_{P_E} m_{\eta_c}^2 \tau^2}{5\xi} + \frac{4m_N m_{P_E} m_{\eta_c}^2 \tau}{5\xi} + \frac{4m_N m_{P_E} m_{\eta_c}^2}{5\xi} - \frac{4}{5} m_N m_{P_E} m_{\eta_c}^2 + \frac{m_{\eta_c}^4 \tau^3}{10\xi} + \frac{2m_{\eta_c}^4 \tau^2}{5\xi} + \frac{2m_{\eta_c}^4 \tau}{5\xi} - \frac{2m_{\eta_c}^4}{5} \quad (\text{A8})$$

$$\kappa_{10} = \frac{m_N^4 m_{P_E}}{5m_{J/\psi}^2 \xi} - \frac{2m_N^2 m_{P_E} \tau}{5\xi} - \frac{4m_N^2 m_{P_E}}{5\xi} - \frac{m_N^5}{5m_{J/\psi}^2 \xi} + \frac{2m_N^3 \tau}{5\xi} + \frac{4m_N^3}{5\xi} - \frac{m_N m_{J/\psi}^2 \tau^2}{5\xi} - \frac{4m_N m_{J/\psi}^2 \tau}{5\xi} - \frac{4m_N m_{J/\psi}^2}{5\xi} \\ + \frac{4m_N m_{J/\psi}^2}{5} + \frac{m_{P_E} m_{J/\psi}^2 \tau^2}{5\xi} + \frac{4m_{P_E} m_{J/\psi}^2 \tau}{5\xi} + \frac{4m_{P_E} m_{J/\psi}^2}{5\xi} - \frac{4m_{P_E} m_{J/\psi}^2}{5} \quad (\text{A9})$$

$$\kappa_{11} = \frac{2m_\Delta^3 m_{P_F}}{15m_{\eta_c}^2 \xi} + \frac{2m_\Delta^2 m_{P_F}}{15m_{\eta_c} \sqrt{\xi}} - \frac{m_{\eta_c}^4 \tau^3}{15m_\Delta^2 \xi} - \frac{2m_{\eta_c}^4 \tau^2}{15m_\Delta^2 \xi} - \frac{2m_\Delta^4}{15m_{\eta_c}^2 \xi} + \frac{2m_{\eta_c}^4 \tau^2}{15m_\Delta^2} + \frac{2m_\Delta^3}{15m_{\eta_c} \sqrt{\xi}} + \frac{m_\Delta^2 \tau}{15\xi} + \frac{4m_\Delta^2}{15\xi} - \frac{4m_\Delta^2}{15} + \frac{2m_{P_F} m_{\eta_c}^2 \tau^2}{15m_\Delta \xi} \\ + \frac{4m_{P_F} m_{\eta_c}^2 \tau}{15m_\Delta \xi} - \frac{4m_{P_F} m_{\eta_c}^2 \tau}{15m_\Delta} - \frac{4m_\Delta m_{P_F} \tau}{15\xi} - \frac{4m_\Delta m_{P_F}}{15\xi} + \frac{4m_\Delta m_{P_F}}{15} - \frac{2m_\Delta m_{\eta_c} \tau}{15\sqrt{\xi}} - \frac{4m_\Delta m_{\eta_c}}{15\sqrt{\xi}} - \frac{2m_{P_F} m_{\eta_c} \tau}{15\sqrt{\xi}} - \frac{4m_{P_F} m_{\eta_c}}{15\sqrt{\xi}} \\ + \frac{2m_{\eta_c}^2 \tau^2}{15\xi} + \frac{2m_{\eta_c}^2 \tau}{15\xi} + \frac{2m_{\eta_c}^2 \tau}{15} + \frac{4m_{\eta_c}^2}{15} \quad (\text{A10})$$

$$\kappa_{12} = -\frac{2m_{P_F} m_{J/\psi}^2 \tau^2}{15m_\Delta^2 \xi} - \frac{4m_{P_F} m_{J/\psi}^2 \tau}{15m_\Delta^2 \xi} + \frac{4m_{P_F} m_{J/\psi}^2 \tau}{15m_\Delta^2} - \frac{2m_{J/\psi}^2 \tau^2}{15m_\Delta \xi} - \frac{4m_{J/\psi}^2 \tau}{15m_\Delta \xi} + \frac{4m_{J/\psi}^2 \tau}{15m_\Delta} + \frac{2m_\Delta \tau}{15\xi} - \frac{4m_\Delta}{15} + \frac{2m_{P_F} \tau}{15\xi} - \frac{4m_{P_F}}{15}$$

## References

- [1] R. Aaij, *et al.*, *Phys. Rev. Lett.* **115**, 072001 (2015) [2] R. Aaij, *et al.*, *Phys. Rev. Lett.* **122**, 222001 (2019)
- [3] R. Aaij, *et al.*, *Phys. Rev. Lett.* **128**, 062001 (2022)

- [4] X. W. Wang and Z. G. Wang, *Chin. Phys. C* **48**, 053102 (2024)
- [5] J. He, *Eur. Phys. J. C* **79**, 393 (2019)
- [6] H. X. Chen, W. Chen, X. Liu, *et al.*, *Phys. Rev. Lett.* **115**, 172001 (2015)
- [7] H. X. Chen, W. Chen and S. L. Zhu, *Phys. Rev. D* **100**, 051501 (2019)
- [8] Z. G. Wang, *Int. J. Mod. Phys. A* **34**, 1950097 (2019)
- [9] M. L. Du, V. Baru, F. K. Guo, *et al.*, *Phys. Rev. Lett.* **124**, 072001 (2020)
- [10] L. Meng, B. Wang, G. J. Wang, *et al.*, *Phys. Rev. D* **100**, 014031 (2019)
- [11] M. Z. Liu, T. W. Wu, M. S. Sanchez, *et al.*, *Phys. Rev. D* **103**, 054004 (2021)
- [12] J. R. Zhang, *Eur. Phys. J. C* **79**, 1001 (2019)
- [13] K. Azizi, Y. Sarac and H. Sundu, *Chin. Phys. C* **45**, 053103 (2021)
- [14] C. W. Xiao, J. Nieves and E. Oset, *Phys. Rev. D* **88**, 056012 (2013)
- [15] H. X. Chen, E. L. Cui, W. Chen, *et al.*, *Eur. Phys. J. C* **76**, 572 (2016)
- [16] M. Z. Liu, F. Z. Peng, M. Sánchez Sánchez, *et al.*, *Phys. Rev. D* **98**, 114030 (2018)
- [17] M. Z. Liu, Y. W. Pan, F. Z. Peng, *et al.*, *Phys. Rev. Lett.* **122**, 242001 (2019)
- [18] C. W. Xiao, J. Nieves and E. Oset, *Phys. Rev. D* **100**, 014021 (2019)
- [19] S. Sakai, H. J. Jing and F. K. Guo, *Phys. Rev. D* **100**, 074007 (2019)
- [20] Z. G. Wang, *Eur. Phys. J. C* **76**, 70 (2016)
- [21] Z. G. Wang, *Int. J. Mod. Phys. A* **35**, 2050003 (2020)
- [22] Z. G. Wang, *Eur. Phys. J. C* **76**, 142 (2016)
- [23] Z. G. Wang, *Int. J. Mod. Phys. A* **36**, 2150071 (2021)
- [24] A. Ali and A. Y. Parkhomenko, *Phys. Lett. B* **793**, 365 (2019)
- [25] R. Zhu, X. Liu, H. Huang, *et al.*, *Phys. Lett. B* **797**, 134869 (2019)
- [26] J. F. Giron, R. F. Lebed and C. T. Peterson, *JHEP* **05**, 061 (2019)
- [27] F. Stancu, *Eur. Phys. J. C* **79**, 957 (2019)
- [28] J. F. Giron and R. F. Lebed, *Phys. Rev. D* **104**, 114028 (2021)
- [29] Y. H. Lin and B. S. Zou, *Phys. Rev. D* **100**, 056005 (2019)
- [30] J. He and D. Y. Chen, *Eur. Phys. J. C* **79**, 887 (2019)
- [31] N. Yalikul, Y. H. Lin, F. K. Guo, *et al.*, *Phys. Rev. D* **104**, 094039 (2021)
- [32] M. Pavon Valderrama, *Phys. Rev. D* **100**, 094028 (2019)
- [33] M. L. Du, V. Baru, F. K. Guo, *et al.*, *JHEP* **08**, 157 (2021)
- [34] F. Z. Peng, L. S. Geng and J. J. Xie, *Phys. Rev. D* **111**, 054029 (2025)
- [35] F. K. Guo, X. H. Liu and S. Sakai, *Prog. Part. Nucl. Phys.* **112**, 103757 (2020)
- [36] H. X. Chen, W. Chen, X. Liu, *et al.*, *Rept. Prog. Phys.* **86**, 026201 (2022)
- [37] L. Meng, B. Wang, G. J. Wang, *et al.*, *Phys. Rept.* **1019**, 2266 (2023)
- [38] Z. G. Wang, *Front. Phys. (Beijing)* **21**, 016300 (2026)
- [39] X. W. Wang, Z. G. Wang, G. L. Yu, *et al.*, *Sci. China Phys. Mech. Astron.* **65**, 291011 (2022)
- [40] X. W. Wang and Z. G. Wang, *Chin. Phys. C* **47**, 013109 (2023)
- [41] Z. G. Wang, *Chin. Phys. C* **45**, 073107 (2021)
- [42] G. J. Wang, L. Y. Xiao, R. Chen, *et al.*, *Phys. Rev. D* **102**, 036012 (2020)
- [43] T. Gutsche and V. E. Lyubovitskij, *Phys. Rev. D* **100**, 094031 (2019)
- [44] Z. G. Wang and X. Wang, *Chin. Phys. C* **44**, 103102 (2020)
- [45] Y. J. Xu, C. Y. Cui, Y. L. Liu, *et al.*, *Phys. Rev. D* **102**, 034028 (2020)
- [46] X. W. Wang and Z. G. Wang, *Int. J. Mod. Phys. A* **37**, 2250189 (2022)
- [47] Z. G. Wang and J. X. Zhang, *Eur. Phys. J. C* **78**, 14 (2018)
- [48] Z. G. Wang, *Eur. Phys. J. C* **79**, 184 (2019)
- [49] Z. G. Wang and Z. Y. Di, *Eur. Phys. J. C* **79**, 72 (2019)
- [50] Z. G. Wang, *Acta Phys. Polon. B* **51**, 435 (2020)
- [51] Z. G. Wang, *Int. J. Mod. Phys. A* **34**, 1950110 (2019)
- [52] Z. G. Wang, H. J. Wang and Q. Xin, *Chin. Phys. C* **45**, 063104 (2021)
- [53] M. A. Shifman, A. I. Vainshtein and V. I. Zakharov, *Nucl. Phys. B* **147**, 385 (1979)
- [54] M. A. Shifman, A. I. Vainshtein and V. I. Zakharov, *Nucl. Phys. B* **147**, 448 (1979)
- [55] L. J. Reinders, H. Rubinstein and S. Yazaki, *Phys. Rept.* **127**, 1 (1985)
- [56] P. Colangelo and A. Khodjamirian, hep-ph/0010175.
- [57] P. A. Zyla *et al.*, *Prog. Theor. Exp. Phys.* **2020**, 083C01 (2020)
- [58] S. Narison and R. Tarrach, *Phys. Lett. B* **125**, 217 (1983)
- [59] Z. G. Wang and T. Huang, *Phys. Rev. D* **89**, 054019 (2014)
- [60] D. Becirevic, G. Duplancic, B. Klajn, *et al.*, *Nucl. Phys. B* **883**, 306 (2014)
- [61] B. L. Ioffe, *Prog. Part. Nucl. Phys.* **56**, 232 (2006)
- [62] Z. G. Wang, *Chin. Phys. C* **46**, 123106 (2022)
- [63] X. W. Wang and Z. G. Wang, *Phys. Rev. D* **110**, 014008 (2024)
- [64] Z. G. Wang, *Phys. Rev. D* **109**, 014017 (2024)
- [65] Z. G. Wang, *Nucl. Phys. B* **993**, 116265 (2023)
- [66] T. J. Burns and E. S. Swanson, *Eur. Phys. J. A* **58**, 68 (2022)
- [67] M. Z. Liu, Y. W. Pan and L. S. Geng, *Phys. Rev. D* **110**, 114022 (2024)
- [68] J. M. Xie, X. Z. Ling, M. Z. Liu, *et al.*, *Eur. Phys. J. C* **82**, 1061 (2022)
- [69] M. B. Voloshin, *Phys. Rev. D* **100**, 034020 (2019)
- [70] Q. Li, C. H. Chang, X. Tong, *et al.*, *JHEP* **10**, 098 (2025)
- [71] Fl. Stancu, *Phys. Rev. D* **104**, 054050 (2021)
- [72] R. Aaij, *et al.*, *Phys. Rev. D* **110**, 032001 (2024)